Author/s:
Bass-Stringer, S;Bernardo, BC;Yildiz, GS;Matsumoto, A;Kiriazis, H;Harmawan, CA;Tai, CMK;Chooi, R;Bottrell, L;Ezeani, M;Donner, DG;D'Elia, AA;Ooi, JYY;Mellett, NA;Luo, J;Masterman, EI;Janssens, K;Olshansky, G;Howden, EJ;Cross, JH;Hagemeyer, CE;Lin, RCY;Thomas, CJ;Magor, GW;Perkins, AC;Marwick, TH;Kawakami, H;Meikle, PJ;Greening, DW;Weeks, KL;La Gerche, A;Tham, YK;McMullen, JR

Title:
Reduced PI3K(p110α) induces atrial myopathy, and PI3K-related lipids are dysregulated in athletes with atrial fibrillation

Date:
2025-12-01

Citation:
Bass-Stringer, S., Bernardo, B. C., Yildiz, G. S., Matsumoto, A., Kiriazis, H., Harmawan, C. A., Tai, C. M. K., Chooi, R., Bottrell, L., Ezeani, M., Donner, D. G., D'Elia, A. A., Ooi, J. Y. Y., Mellett, N. A., Luo, J., Masterman, E. I., Janssens, K., Olshansky, G., Howden, E. J. ,... McMullen, J. R. (2025). Reduced PI3K(p110α) induces atrial myopathy, and PI3K-related lipids are dysregulated in athletes with atrial fibrillation. Journal of Sport and Health Science, 14, pp.101023-. https://doi.org/10.1016/j.jshs.2025.101023.

Persistent Link:
https://hdl.handle.net/11343/359740

HOSTED BY

ELSEVIER

Available online at www.sciencedirect.com

ScienceDirect

Journal of Sport and Health Science

Original article

Reduced PI3K(p110α) induces atrial myopathy, and PI3K-related lipids are dysregulated in athletes with atrial fibrillation

Sebastian Bass-Stringer [a,b], Bianca C. Bernardo [a,c,d], Gunes S. Yildiz [a], Aya Matsumoto [a], Helen Kiriazis [a,e], Claudia A. Harmawan [a], Celeste M.K. Tai [a], Roger Chooi [a], Lauren Bottrell [a], Martin Ezeani [a], Daniel G. Donner [a,e], Aascha A. D'Elia [a], Jenny Y.Y. Ooi [a], Natalie A. Mellett [a], Jieting Luo [a], Emma I. Masterman [a], Kristel Janssens [a], Gavriel Olshansky [a,e], Erin J. Howden [a,e], Jonathon H. Cross [a], Christoph E. Hagemeyer [f], Ruby C.Y. Lin [g,h], Colleen J. Thomas [b,i], Graham W. Magor [f], Andrew C. Perkins [f], Thomas H. Marwick [a,e,j,k], Hiroshi Kawakami [a,l], Peter J. Meikle [a,e,i], David W. Greening [a,e,m], Kate L. Weeks [a,c,e,n], André La Gerche [a,e], Yow Keat Tham [a,c,e,m], Julie R. McMullen [a,b,c,e,m,o,p,*]

[a] *Baker Heart and Diabetes Institute, Melbourne, VIC 3004, Australia*
[b] *Department of Physiology, Anatomy and Microbiology, La Trobe University, Bundoora, VIC 3086, Australia*
[c] *Department of Diabetes, Central Clinical School, Monash University, Clayton, VIC 3800, Australia*
[d] *Department of Paediatrics, University of Melbourne, Melbourne, VIC 3010, Australia*
[e] *Department of Cardiometabolic Health, University of Melbourne, Melbourne, VIC 3010, Australia*
[f] *Australian Centre for Blood Diseases, Monash University, Clayton, VIC 3800, Australia*
[g] *School of Medical Sciences, University of NSW, Sydney, NSW 2052, Australia*
[h] *Westmead Institute for Medical Research, Sydney, NSW 2145, Australia*
[i] *Centre for Cardiovascular Biology and Disease Research, La Trobe University, Bundoora, VIC 3086, Australia*
[j] *Menzies Institute for Medical Research, University of TAS, Hobart, TAS 7000, Australia*
[k] *Department of Cardiology, Royal Hobart Hospital, Hobart, TAS 7001, Australia*
[l] *Department of Cardiology, Pulmonology, Hypertension, and Nephrology, Ehime University Graduate School of Medicine, Toon 791-0295, Japan*
[m] *Department of Cardiovascular Research, Translation and Implementation, La Trobe University, Bundoora, VIC 3086, Australia*
[n] *Department of Anatomy & Physiology, University of Melbourne, Melbourne, VIC 3010, Australia*
[o] *Department of Physiology and Department of Medicine Alfred Hospital, Monash University, Clayton, VIC 3800, Australia*
[p] *Heart Research Institute, Newtown, NSW 2042, Australia*

Received 19 July 2024; revised 11 November 2024; accepted 10 December 2024
Available online 16 January 2025

Abstract

Background: Elucidating mechanisms underlying atrial myopathy, which predisposes individuals to atrial fibrillation (AF), will be critical for preventing/treating AF. In a serendipitous discovery, we identified atrial enlargement, fibrosis, and thrombi in mice with reduced phosphoinositide 3-kinase (PI3K) in cardiomyocytes. PI3K(p110α) is elevated in the heart with exercise and is critical for exercise-induced ventricular enlargement and protection, but the role in the atria was unknown. Physical inactivity and extreme endurance exercise can increase AF risk. Therefore, our objective was to investigate whether too little and/or too much PI3K alone induces cardiac pathology.

Methods: New cardiomyocyte-specific transgenic mice with increased or decreased PI3K(p110α) activity were generated. Multi-omics was conducted in mouse atrial tissue, and lipidomics in human plasma.

Results: Elevated PI3K led to an increase in heart size with preserved/enhanced function. Reduced PI3K led to atrial dysfunction, fibrosis, arrhythmia, increased susceptibility to atrial enlargement and thrombi, and dysregulation of monosialodihexosylganglioside (GM3), a lipid that regulates insulin-like growth factor-1 (IGF1)−PI3K signaling. Proteomic profiling identified distinct signatures and signaling networks across

Peer review under responsibility of Shanghai University of Sport.
* Corresponding author.
E-mail address: julie.mcmullen@hri.org.au (J.R. McMullen).

https://doi.org/10.1016/j.jshs.2025.101023
Cite this article: Bass-Stringer S, Bernardo BC, Yildiz GS, et al. Reduced PI3K(p110α) induces atrial myopathy, and PI3K-related lipids are dysregulated in athletes with atrial fibrillation. *J Sport Health Sci* 2025;14:101023.

atria with varying degrees of dysfunction, enlargement, and thrombi, including commonalities with the human AF proteome. PI3K-related lipids were dysregulated in plasma from athletes with AF.
Conclusion: PI3K(p110α) is a critical regulator of atrial biology and function in mice. This work provides a proteomic resource of candidates for further validation as potential new drug targets and biomarkers for atrial myopathy. Further investigation of PI3K-related lipids as markers for identifying individuals at risk of AF is warranted. Dysregulation of PI3K may contribute to the association between increased cardiac risk with physical inactivity and extreme endurance exercise.

Keywords: Atrial myopathy; Atrial fibrillation; Lipidomics; Proteomics; Exercise

1. Introduction

The prevalence of atrial fibrillation (AF) continues to increase globally due to an aging population and risk factors including physical inactivity, obesity, type 2 diabetes, and hypertension. Despite significant research and strategies to prevent and treat AF, this condition remains very challenging.[1,2] Understanding mechanisms underlying atrial myopathy, fibrosis, and atrial thrombi formation will be critical for preventing and treating AF, stroke, and heart failure.[3] The current study arose from (a) a serendipitous discovery in cardiac-specific transgenic mice with reduced phosphoinositide 3-kinase (PI3K) p110α presenting with atrial enlargement, atrial fibrosis, and atrial thrombi, and (b) our interest in understanding the dose−response and therapeutic potential of PI3K-based drugs. PI3K is a critical regulator of exercise-induced cardiac protection and enlargement (physiological hypertrophy)[4,5] that can both prevent and restore cardiac function in mice in cardiac disease settings.[5−10] While the importance of physical activity and exercise for cardiovascular health is well-established,[11−13] there are also reports that long-term extreme exercise can lead to increased risk of cardiac pathology.[14,15] With both physical inactivity and extreme activity being linked to elevated cardiac risk, a U- or reverse J-shaped relationship between exercise and cardiac health has been proposed. While the "extreme exercise hypothesis" remains controversial, there is a growing body of evidence demonstrating that high volumes of extreme endurance exercise are associated with an increased risk of atrial pathology and AF.[14−19] Further, there is evidence that long term overexpression of an upstream regulator of PI3K, insulin-like growth factor 1 (IGF1), contributes to cardiac pathology, including atrial enlargement.[20] Given the IGF1−PI3K−protein kinase B (Akt) pathway is a critical molecular pathway increased in the heart in response to exercise,[21,22] to evaluate its potential as a therapeutic target or biomarker, it is essential to assess the "safety profile" and "therapeutic window" of this pathway.

Our previous work showed that cardiac-specific heterozygote transgenic (Tg) mice with reduced PI3K activity, due to the expression of a dominant-negative PI3K (dnPI3K) mutant on 1 allele (dnPI3K Tg(+/−)), had smaller hearts with normal heart function under basal conditions.[23] The dnPI3K Tg(+/−) mice displayed a blunted hypertrophic response to exercise training,[24] highlighting the critical role of PI3K for exercise-induced cardiac enlargement. Conversely, heterozygote Tg mice with increased cardiac PI3K activity, due to a constitutively activated PI3K mutant (caPI3K Tg(+/−)), displayed a physiological hypertrophic phenotype under basal conditions[23] and were protected following myocardial infarction (MI), dilated cardiomyopathy (DCM), and pressure overload.[5,6,10] When we unintentionally generated homozygote dnPI3K Tg mice (dnPI3K Tg(+/+)) due to a breeding error, we found atrial enlargement and thrombi in a subset of dnPI3K Tg(+/+) mice. The first goal of this study was to generate and characterize both heterozygote and homozygote PI3K Tg mice to (a) assess whether the finding of atrial pathology in homozygote dnPI3K Tg was reproducible, (b) examine whether a further increase in PI3K activity in homozygote caPI3K Tg mice illustrates a dose−response curve for physiological hypertrophy or crosses a protective threshold, leading to cardiac pathology and arrhythmia, as seen in some athletes undertaking extreme exercise, and (c) assess whether mice with varying degrees of atrial dysfunction, pathology, and atrial thrombi exhibit a distinct atrial proteome signature. The next goal was to assess the translational potential by comparing the mouse atrial proteome with the human AF proteome and measuring PI3K-related lipids in individuals with AF.

2. Materials and methods

2.1. Ethics approvals

Animal care and experimental procedures were approved by the Alfred Research Alliance Animal Ethics Committee and performed in accordance with the Australian Code for the Care and Use of Animals for Scientific Purposes (National Health and Medical Research Council (NHMRC), 8th edition, 2013) and conform to the National Institutes of Health (NIH) Guide for the Care and Use of Laboratory Animals. Mice were euthanized by i.p. injection of pentobarbitone (300−400 mg/kg; Virbac, Milperra, NSW, Australia) and cervical dislocation.

Studies in plasma samples collected from veteran athletes with or without AF from the ProAFheart study (Australian New Zealand Clinical Trials Registry, ACTRN12618000711213) were approved by the Alfred Hospital Human Ethics Committee (HREC/16/Alfred/156, Melbourne, VIC, Australia), conforming to the principles outlined in the Declaration of Helsinki. All patients gave written informed consent to the collection of samples.

2.2. Generation of homozygote PI3K Tg mouse models

Two new genetic mouse models (homozygote PI3K Tg with increased or decreased PI3K(p110α) activity) were generated from previously described cardiac-specific heterozygote

PI3K transgenic mice (i.e., heterozygote caPI3K Tg (caPI3K Tg(+/−)) with increased PI3K(p110α) activity and heterozygote dnPI3K Tg (dnPI3K Tg(+/−)) with decreased PI3K (p110α) activity).[23] The caPI3K and dnPI3K Tg mice were generated using the α-myosin heavy chain (αMHC) promoter to drive transgene expression in cardiac myocytes only.[23] Expression of the constitutively active PI3K construct (a chimeric molecule that contains the iSH2 domain of p85 fused to the N-terminus of p110α by a glycine linker) was associated with increased cardiac PI3K activity, increased heart size, and increased cardiac myocyte size in the heterozygote mice. In contrast, the dnPI3K construct (truncated p110 lacking the kinase domain) was associated with reduced PI3K activity, reduced heart size, and reduced myocyte size.[23] The new models generated were homozygote Tg (i.e., caPI3K Tg(+/+) and dnPI3K Tg(+/+)). Further details including evidence of PI3K(p110α) mediating the phenotype in dnPI3K Tg mice as well as information regarding genotyping and animal exclusions[25] are provided in the Supplementary Methods.

2.3. Experimental techniques

Studies were performed in mature adult mice at ∼20 or 30−32 week of age. Details of assessment of (a) left ventricular (LV) and atrial dimensions and function in anaesthetized mice (isoflurane; Lyppard, Moorabbin Airport, VIC, Australia, inhalation: 3.5%−4.0% induction, 1.6%−2.0% maintenance) by echocardiography and electrical activity by electrocardiogram (ECG), (b) isolation of adult cardiac myocytes using the Langendorff apparatus, (c) assessment of fibrosis by histological analysis, (d) molecular/omics analyses (gene expression, PI3K activity assays, proteomics, and lipidomics) are provided in the Supplementary Methods. This includes mouse tissues and plasma from veteran athletes with or without AF (ProAF-heart study). The athletes (>40 years) had been engaged in endurance sports training and competition for >10 years (e.g., rowing, triathlon, cycling, and cross-country skiing).

2.4. Statistics

Statistical analysis was performed using GraphPad Prism Version 7/10 (GraphPad Software, La Jolla, CA, USA), unless otherwise specified. Results are shown as the mean ± standard error of the mean (SEM), unless otherwise stated. Differences between groups were determined using one-way analysis of variance (ANOVA) followed by Tukey's range test or Mann−Whitney *U*-test if data were not normally distributed (as assessed by Shapiro−Wilk normality test). Unpaired *t* tests were used to compare 2 groups. A value of $p < 0.05$ was considered significant, unless otherwise stated. All tests were two-sided. Statistics related to proteomic and lipidomic analyses are provided in the Supplementary Methods.

3. Results

This study represents the first generation and characterization of cardiac-specific homozygote PI3K Tg mice (caPI3K Tg(+/+) and dnPI3K Tg(+/+)) in comparison to heterozygotes (caPI3K Tg(+/−) and dnPI3K Tg(+/−)) and non-transgenic (Ntg) littermate controls. First, we confirmed that PI3K activity and/or PI3K regulatory protein expression and feedback signaling on the IGF1 receptor (IGF1R) was regulated in a dose−response manner (i.e., greatest in caPI3K Tg(+/+) and lowest in dnPI3K Tg(+/+)) (Supplementary Fig. 1).

3.1. caPI3K Tg mice display cardiac hypertrophy in a dose-dependent manner and have preserved/enhanced systolic function

Heart size and normalized heart weight (HW)/body weight (BW) and HW/tibia length (TL) ratios of adult male and female caPI3K Tg(+/−) mice (∼20 week) were increased *vs*. Ntg (Fig. 1A−1C and Supplementary Table 1). A further increase in heart size was identified in caPI3K Tg(+/+) *vs*. caPI3K Tg(+/−) (Fig. 1A−1C), indicative of higher PI3K activity inducing a greater hypertrophic response. Atrial weight (AW)/TL was modestly lower in male caPI3K Tg(+/−) *vs*. Ntg but not different in other groups (Fig. 1D and Supplementary Table 1). Lung weight (LW)/TL was comparable in all groups (Fig. 1E), with no evidence of congestion or pathology. By echocardiography, LV posterior wall (LVPW) and interventricular septum (IVS) thicknesses, and estimated LV mass were significantly increased or tended to be increased in both caPI3K Tg models *vs*. Ntg (Fig. 1F and Supplementary Table 2). LV systolic function (fractional shortening) was preserved or enhanced in both caPI3K Tg models (Fig. 1F). Diastolic parameters were comparable between groups (Supplementary Table 3). Pressure-volume (PV) loop parameters showed no differences between groups (Supplementary Table 4), and there was no evidence of electrophysiological abnormalities *vs*. Ntg based on ECG parameters or arrhythmia (any irregularities in cardiac rhythm < 4.5% of total time) (Fig. 1G and Supplementary Table 5).

3.2. Homozygote dnPI3K Tg mice display cardiac dysfunction, arrhythmia, and atrial pathology

Our previous characterization of dnPI3K Tg(+/−) showed that reduced cardiac PI3K resulted in mice with smaller hearts but relatively normal heart function.[23,26] In the current study, heterozygote and homozygote dnPI3K Tg had smaller heart weights *vs*. Ntg, but there was no difference between the heterozygotes and homozygotes (Fig. 2A−2C and Supplementary Table 6). Given the absence of a dose−response effect of the dnPI3K transgene on heart weight, we evaluated the impact on cardiac myocyte size by isolating adult cardiac myocytes. The cell area and length of cardiac myocytes from dnPI3K Tg (+/−) were smaller than Ntg and further reduced in dnPI3K Tg (+/+) (Fig. 2D and Supplementary Fig. 2A). Consistent with the smaller heart weight, dnPI3K Tg(+/−) also had smaller AW *vs*. Ntg (Fig. 2E and Supplementary Table 6), and the AW/HW ratio was comparable to Ntg (Fig. 2F). By contrast, dnPI3K Tg(+/+) had greater AW than dnPI3K Tg(+/−) and a higher AW/HW ratio *vs*. Ntg and dnPI3K Tg(+/−) (Fig. 2E and 2F), and there was notable evidence of atrial fibrosis in dnPI3K Tg(+/+) but not the other groups (Fig. 2G, collagen

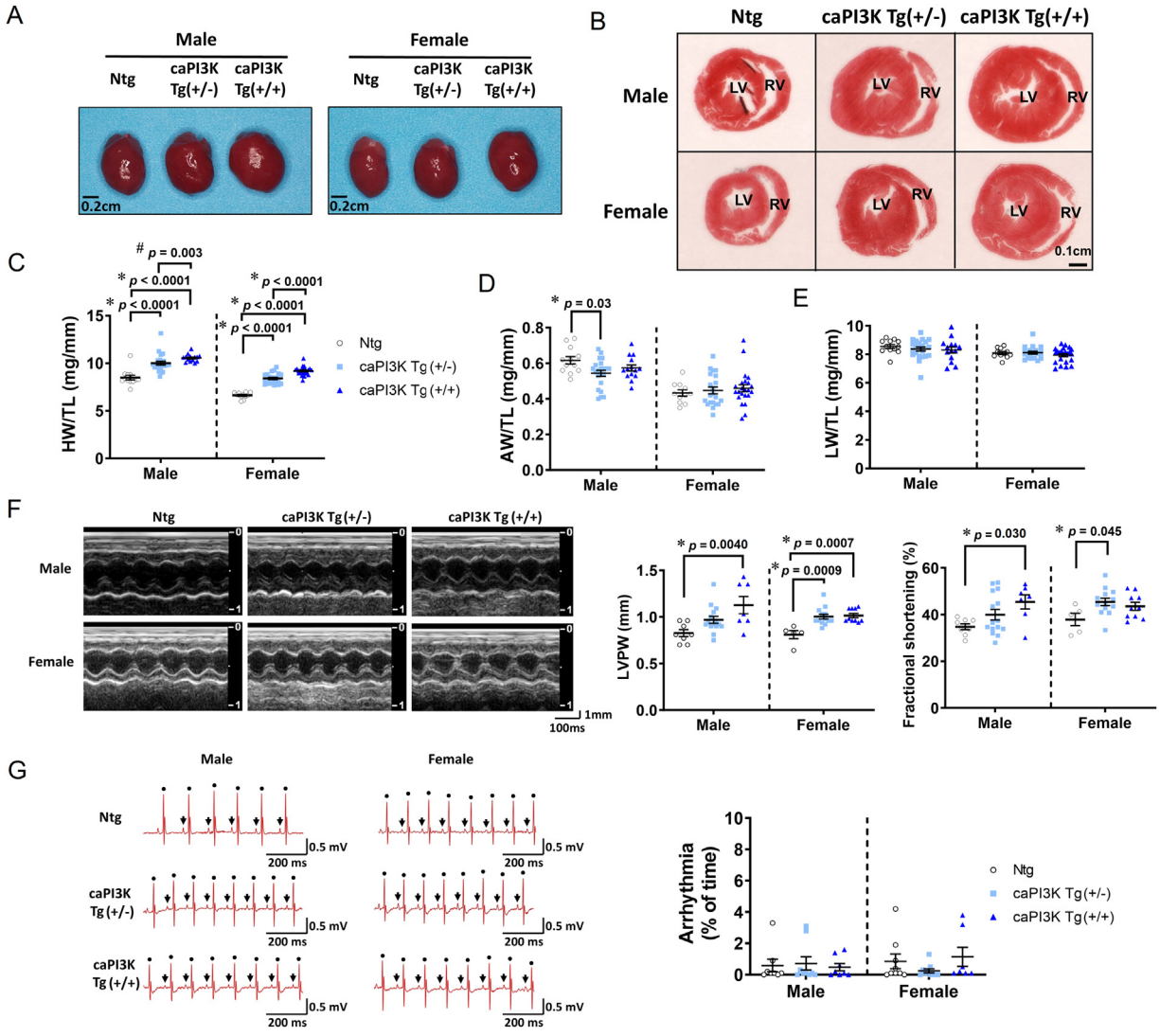

Fig. 1. Dose-dependent increase in heart size of caPI3K Tg mice and normal/enhanced heart function. (A) Hearts of male and female Ntg, heterozygote caPI3K Tg (+/−), and homozygote caPI3K Tg(+/+) mice at dissection. All data in the figure come from mice at ∼20 week of age. (B) Representative ventricular sections. (C−E) HW, AW, and LW normalized to TL. Ntg (male/female): $n = 12/11$, caPI3K Tg(+/−): $n = 22/21$, caPI3K Tg(+/+): $n = 14/23$. (F) M-mode echocardiographic images. LVPW and percentage of fractional shortening (%). Ntg (male/female): $n = 8/5$, caPI3K Tg(+/−): $n = 15/13$, caPI3K Tg(+/+): $n = 7/10$. (G) Left, electrocardiogram traces. Dots and arrows highlight R- and P-waves, respectively. Right, episodes of arrhythmia expressed as a percentage over an interval of ∼5−6 min (further details in Supplementary Methods). Ntg (male/female): $n = 8/9$, caPI3K Tg(+/−): $n = 9/10$, caPI3K Tg(+/+): $n = 8/7$. Data points represent individual mice, presented as mean ± standard error of the mean (SEM). * indicates the one way analysis of variance followed by correction for multiple comparisons using Tukey's method. # *p*-value by Mann-Whitney *U*-test *vs*. caPI3K Tg(+/−) of same sex. AW = atrial weight; caPI3K Tg(+/−) = heterozygote constitutively activated phosphoinositide 3-kinase mutant; caPI3K Tg(+/+) = homozygote constitutively activated phosphoinositide 3-kinase mutant; HW = heart weight; LV = left ventricle; LVPW = left ventricular posterior wall thickness; LW = lung weight; Ntg = non-transgenic; RV = right ventricle; TL = tibia length.

fibers stain blue). Atrial thrombi were identified in 7 of 34 dnPI3K Tg(+/+) but no thrombi were found in Ntg or dnPI3K Tg(+/−) (Fig. 2H).

LV wall thicknesses and estimated LV mass were measured by echocardiography and were generally lower in dnPI3K Tg groups, and fractional shortening was lower in dnPI3K Tg (+/+) *vs*. Ntg and dnPI3K Tg(+/−) (Fig. 2I and Supplementary Table 7). In males, pressure parameters, contractility, and stroke work were lower in dnPI3K Tg(+/+) *vs*. Ntg; there were no differences in dnPI3K Tg(+/−) (Fig. 2J, Supplementary Fig. 2B and 2C, and Supplementary Table 8). In female dnPI3K Tg(+/−), some pressure and volume parameters tended to be lower *vs*. Ntg, and this translated into a significant fall in stroke work. Measures of pressure, volume, contractility, and stroke work were all significantly lower in female dnPI3K Tg(+/+) *vs*. Ntg (Fig. 2J, Supplementary Fig. 2B and 2C, and Supplementary Table 8). As previously reported,[26] ECG parameters were relatively normal in dnPI3K Tg(+/−) *vs*. Ntg (Fig. 2K). However, there was evidence of some arrhythmia in dnPI3K Tg(+/−), particularly in females (Fig. 2K). In dnPI3K Tg(+/+) there were prominent ECG abnormalities, including irregular R−R intervals and arrhythmia (Fig. 2K and 2L, Supplementary Fig. 2D, and Supplementary Table 9).

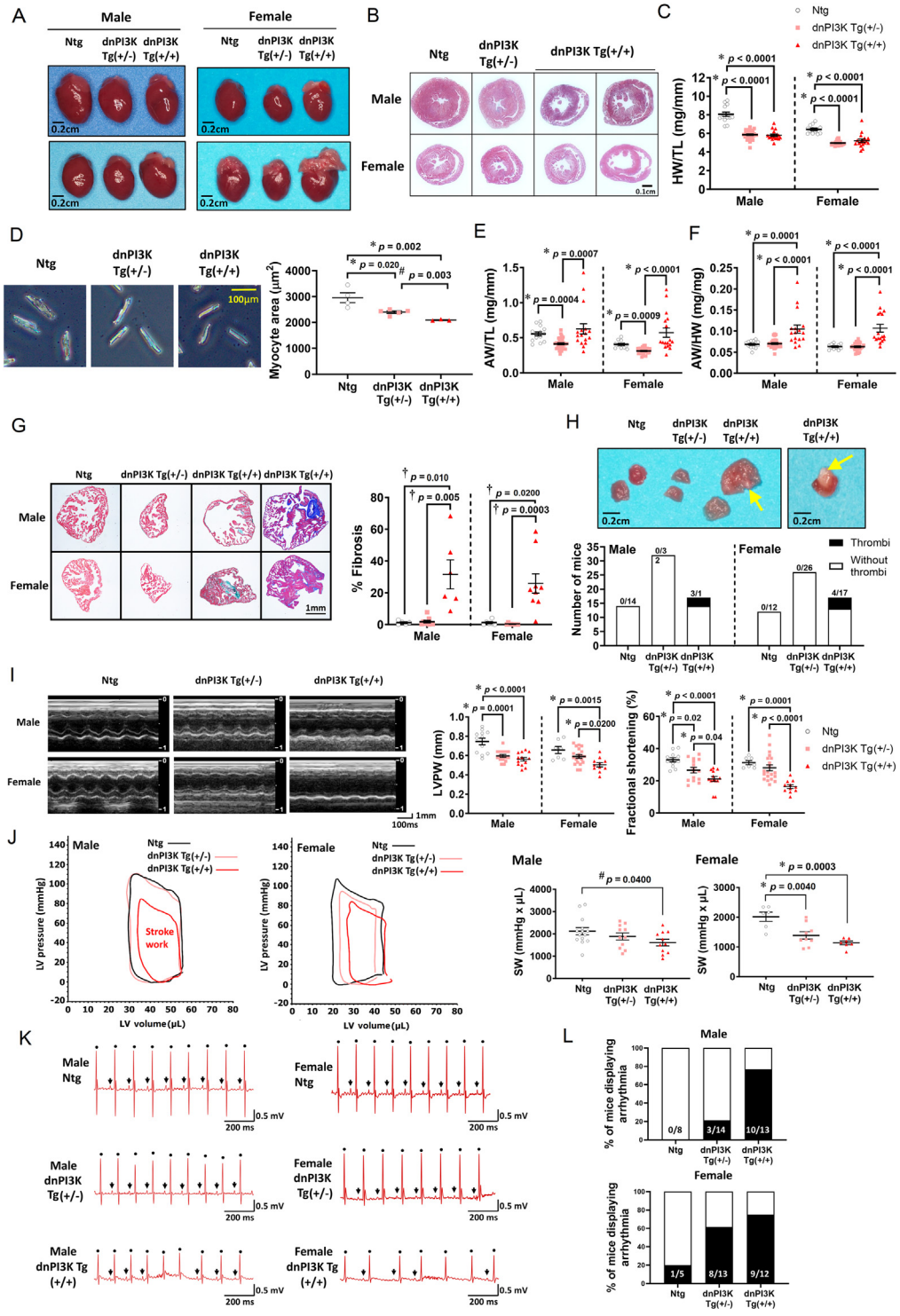

Fig. 2. Distinct morphological phenotypes of heterozygote and homozygote dnPI3K Tg mice. (A) Hearts of male and female Ntg, heterozygote dnPI3K Tg(+/−), and homozygote dnPI3K Tg(+/+) mice at dissection. Images from the homozygote Tg highlight the range of phenotypes (i.e., dilated chambers and enlarged atria). All data presented in the figure come from mice at ∼20 week of age, unless otherwise stated. (B) Ventricular cross-sections. Unlike the Ntg and dnPI3K Tg(+/−), the dnPI3K Tg(+/+) presented with varying phenotypes (A and B—i.e., a subset of dnPI3K Tg(+/+)—had more dilated hearts at dissection (right). (C) HW normalized to TL. (D) Images of isolated ventricular myocytes and quantitation of myocyte area from male Ntg ($n = 4$), dnPI3K Tg(+/−) ($n = 5$), dnPI3K Tg(+/+) ($n = 3$), respectively. AW normalized to (E) TL and (F) HW. (C, E, and F): Ntg (male/female): $n = 14/12$, dnPI3K Tg(+/−): $n = 32/26$, dnPI3K Tg(+/+): $n = 17/17$. (G) LA samples stained with Masson's Trichrome showing atrial fibrosis (blue) in the dnPI3K Tg(+/+) mice and quantitation. Ntg (male/female): $n = 5/6$, dnPI3K Tg (+/−): $n = 9/9$, dnPI3K Tg(+/+): $n = 6/9$. (H) Upper, photos at dissection of atria from female mice (yellow arrows highlight thrombi). Lower, number of mice presenting with atrial thrombi at dissection. (I) M-mode echocardiographic measurements. LVPW thickness and percentage of fractional shortening (%). Ntg (male/female): $n = 12/7$, dnPI3K Tg(+/−): $n = 15/20$, dnPI3K Tg(+/+): $n = 13/11$. (J) P−V loop analysis curves and quantitation of SW in mice at ∼32 week. Ntg (male/female): $n = 14/6$, dnPI3K Tg(+/−): $n = 11/9$, dnPI3K Tg(+/+): $n = 11/7$. (K) Electrocardiogram traces. Dots and arrows highlight R and clear P-waves,

3.3. Distinct histological and molecular profiles in caPI3K Tg and dnPI3K Tg mice

Fibrosis was not evident in LV from heterozygote or homozygote caPI3K Tg (Supplementary Fig. 3A) or heterozygote dnPI3K Tg (Supplementary Fig. 3B). By contrast, fibrosis was present in LV from male and female dnPI3K Tg(+/+) (Supplementary Fig. 3B). Genes commonly altered in a setting of pathological hypertrophy (*natriuretic peptide A* (*Nppa*): encoding atrial natriuretic peptide (ANP), *natriuretic peptide B* (*Nppb*): encoding B-type natriuretic peptide (BNP)) were not different or were decreased in the ventricles of caPI3K Tg groups (Supplementary Fig. 3C) but were increased in the dnPI3K Tg(+/−) and dnPI3K Tg(+/+) (Supplementary Fig. 3D), progressively for ANP. Collagen genes (*collagen type I alpha 1 chain* (*Col1a1*) and *collagen type III alpha 1 chain* (*Col3a1*)) were elevated in the ventricles of the dnPI3K Tg models (Supplementary Fig. 3E), generally highest in the dnPI3K Tg(+/+), consistent with the histological analysis (Supplementary Fig. 3B). Gene expression of *ATPase sarcoplasmic/endoplasmic reticulum Ca^{2+} transporting 2* (*Atp2a2*) (encodes sarcoplasmic/endoplasmic reticulum Ca^{2+} ATPase 2a (Serca2a)) was depressed in male and female dnPI3K Tg (+/+) ventricles (Supplementary Fig. 3F), and this corresponded with systolic dysfunction in homozygote dnPI3K Tg (Fig. 2I). Collagen genes and Serca2a were largely unchanged in the caPI3K Tg models (Supplementary Fig. 3G and 3H).

3.4. Transgene integration of dnPI3K did not disrupt coding sequence, and expression of the dnPI3K mutant protein was not excessively elevated

The injection of foreign DNA into the pronucleus of zygotes to produce transgenic mice has the potential to disrupt the coding sequence of endogenous genes and cause non-specific phenotypes.[27] Given the unexpected observation of atrial pathology and thrombi in the dnPI3K Tg(+/+), we performed targeted locus amplification (TLA) analysis, a method that identifies the insertion site through deep sequencing of genomic loci linked to specific known transgene cassettes. This analysis showed that the transgene was inserted towards the end of chromosome 16 in an intergenic region. There was an associated deletion of ∼85 kb at the integration site (Supplementary Fig. 4A and 4B). Given the dnPI3K transgene did not disrupt any known coding sequence and is ∼500 kb from the nearest gene there is no obvious evidence the phenotype is due to an unwanted genomic disruption.

In some transgenic models, very high expression of a mutant protein can lead to non-specific phenotypes. Both the caPI3K and dnPI3K mutant proteins can be assessed by Western blotting using an antibody that detects endogenous PI3K(p110α). The caPI3K mutant is larger than endogenous PI3K (∼150 kDa, a chimeric molecule that contains the iSH2 domain of p85 fused to the N-terminus of p110α by a glycine linker), and the dnPI3K mutant is smaller (∼73 kDa, truncated p110 lacking the kinase domain). The expression of the mutant proteins in the atria of the PI3K Tg was not excessive in comparison to endogenous PI3K(p110α) in the atria of Ntg (Supplementary Fig. 4C; ∼2−4 fold). Further, given expression of the mutants was comparable in atria of dnPI3K Tg (+/+) and caPI3K Tg(+/+) mice (Supplementary Fig. 4C), and the caPI3K homozygous mice displayed no cardiac pathology, it is unlikely that the phenotype in the dnPI3K homozygous mice is due to high expression of the mutant protein.

3.5. Reduced PI3K is associated with atrial dysfunction in heterozygote and homozygote dnPI3K Tg

Next, we undertook a detailed assessment of atrial dimensions and function by echocardiography in additional cohorts of dnPI3K Tgs. Atrial dysfunction was identified in heterozygote mice *vs*. Ntg based on multiple parameters including left atrium (LA) reservoir function, LA booster pump function, and LA and appendage/RA emptying fractions (Fig. 3 and Supplementary Table 10). The degree of atrial dysfunction in heterozygotes appeared to be more pronounced than the ventricular dysfunction in the same mice based on LV ejection fraction (Supplementary Table 11). Comparable or further atrial dysfunction was identified in the homozygotes (Fig. 3 and Supplementary Table 10) *vs*. heterozygotes. Atrial area and volume data (Supplementary Table 10) showed significant increases in female dnPI3K Tg(+/+) *vs*. Ntg, with a similar non-significant pattern in males. Unexpectedly, atrial areas and volumes were not lower in heterozygote dnPI3K *vs*. Ntg, despite atrial weights being lower (Fig. 2E). To assess this further, we acquired video recordings. *In situ*, dnPI3K Tg (+/−) had atria that expanded to a comparable degree to dnPI3K Tg(+/+) and more than Ntg (Supplementary Data File 1). We conclude that dnPI3K Tg(+/−) atria expand more than Ntg *in vivo*, but reduced atrial wall thickness in dnPI3K Tg (+/−) in the absence of obvious fibrosis explains the smaller atrial weights *vs*. Ntg.

3.6. Mechanisms underlying atrial fibrosis, enlargement, and atrial thrombi in homozygote dnPI3K

To understand the potential mechanisms contributing to pathology within the atria from dnPI3K Tg(+/+), but also the varying phenotypes (i.e., some mice presenting with enlarged atria and thrombi), we performed quantitative proteomic analyses on the right atrium (RA) from 5 groups of female mice: Ntg, dnPI3K Tg(+/−), and 3 subsets of dnPI3K Tg(+/+) with

respectively. (L) Percentage of mice displaying arrhythmia during an interval of ∼5−6 min. The threshold for selecting mice displaying arrhythmia was set at >4.5% based on data obtained from Ntg mice in Fig. 1H (further details in Supplementary Methods). Numbers within the bar graphs refer to the number of mice displaying arrhythmia. Ntg (male/female): $n = 8/5$, dnPI3K Tg(+/−): $n = 14/13$, dnPI3K Tg(+/+): $n = 13/12$. Data points represent individual mice, presented as mean ± SEM. * indicates the one way analysis of variance followed by Tukey's. † indicates Kruskal-Wallis followed by Dunn's (data not normally distributed). # *p* value by unpaired *t* test. AW = atrial weight; dnPI3K Tg(+/−) = heterozygote dominant-negative phosphoinositide 3-kinase mutant; dnPI3K Tg(+/+) = homozygote dominant-negative phosphoinositide 3-kinase mutant; HW = heart weight; LA = left atrium; LVPW = left ventricular posterior wall thickness; Ntg = non-transgenic; SW = stroke work; TL = tibial length.

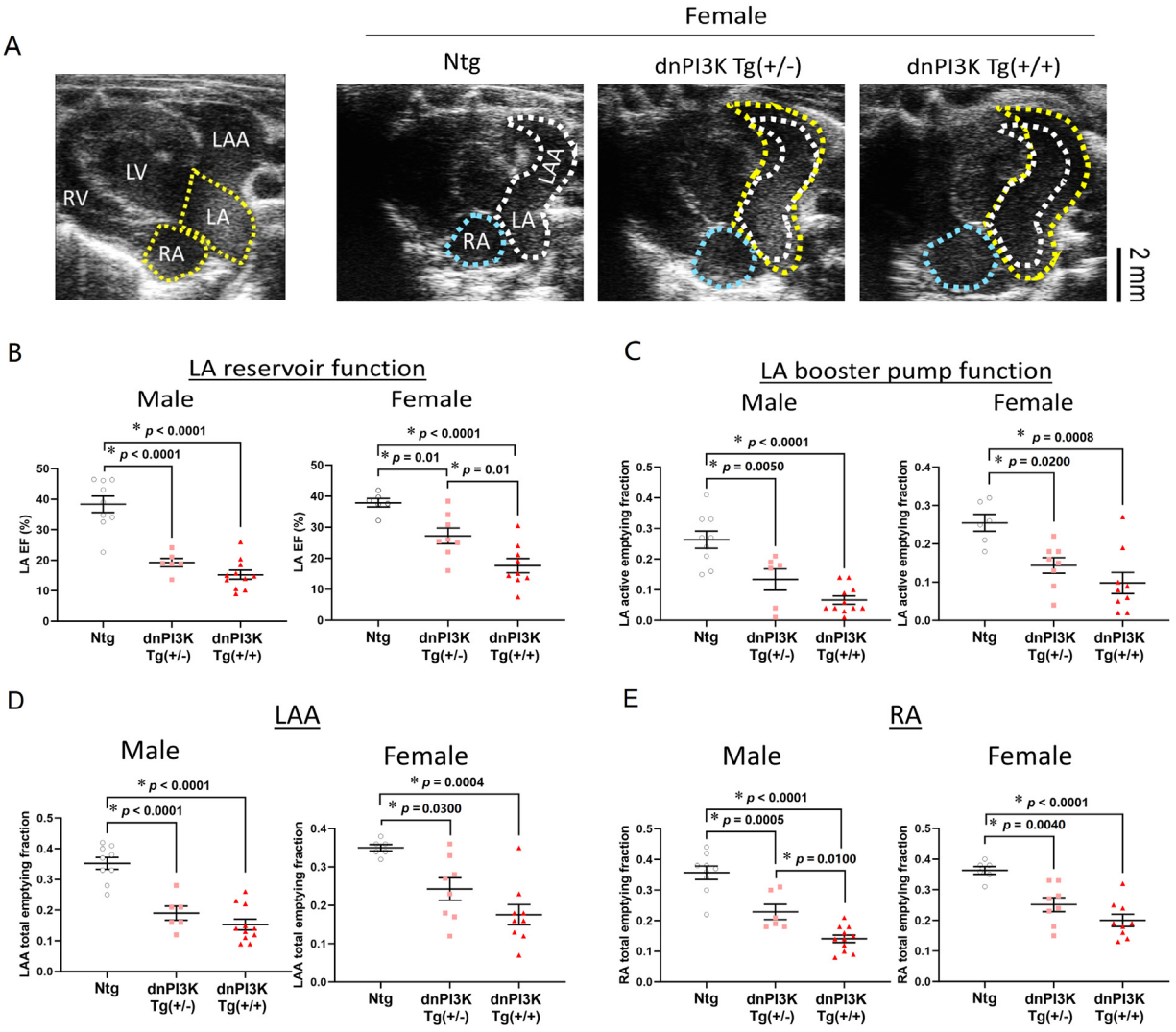

Fig. 3. Atrial dysfunction in heterozygote and homozygote dnPI3K Tg models. (A) Left panel, echocardiographic image highlighting the location of the mouse LA, LAA, RA, LV, and RV. Right panel, representative images from female mice. Trace from Ntg (white) superimposed onto dnPI3K Tg(+/−)/Tg(+/+) shown in yellow. (B−E) Measurements from (B) LA reservoir function, (C) LA Booster pump fuction, (D) LAA, and (E) RA of male and female mice at ∼30 week. Ntg (male/female): $n = 9/6$, dnPI3K Tg(+/−): $n = 6/8$, dnPI3K Tg(+/+): $n = 11/9$. Data points represent individual mice, presented as mean ± SEM. * indicates the one way analysis of variance followed by Tukey's. dnPI3K Tg(+/−) = heterozygote dominant-negative phosphoinositide 3-kinase mutant; dnPI3K Tg(+/+) = homozygote dominant-negative phosphoinositide 3-kinase mutant; EF = ejection fraction; LA = left atrium; LAA = LA appendage; LV = left ventricular; Ntg = non-transgenic; RA = right atrium; RV = right ventricle.

different phenotypes based on atrial mass. Female mice and the RA were used because they presented with the broadest spectrum of phenotypes based on atrial enlargement (Fig. 2E). For the 3 subsets of dnPI3K Tg(+/+), we selected mice with total atria weight <7 mg (similar weight to dnPI3K Tg(+/−), designated "S" for small), 7−10 mg (similar weight to Ntg, designated "M" for medium), and >10 mg (weight greater than Ntg and dnPI3K Tg(+/−), designated "L" for large) (Fig. 4A). First, we compared the proteome of all 5 groups together. Of the 5700 total proteins identified, 4381 proteins were identified across all groups. While there were differences between the 5 groups (Fig. 4B and 4C), the heatmap and principle component analysis (PCA) showed the most distinct clustering in the dnPI3K Tg(+/+) L group (Fig. 4B and 4D and Supplementary Data File 2). Gene Ontology enrichment analysis highlighted 3 main clusters within the heatmap (Fig. 4B and 4E−4G) showing upregulated protein networks (Cluster 723: e.g., negative regulation of cellular metabolic process, elastic fiber assembly) and downregulated protein networks (Cluster 724: e.g., muscle structure development, muscle contraction, sarcomere organization; Cluster 725: e.g., metabolic processes and pathways). Given the distinct phenotypic differences between other groups (e.g., Ntg and dnPI3K Tg(+/−)), we proceeded to compare the proteome of groups without the dnPI3K Tg(+/+) L group, which may have been dominating the analysis and masking more subtle differences. PCA and heatmap analysis showed differences between Ntg and dnPI3K Tg(+/−) (Supplementary Fig. 5), dnPI3K Tg (+/−) and dnPI3K Tg(+/+) S (Supplementary Fig. 6). A comparison of all 3 dnPI3K Tg(+/+) groups (S, M, and L)

highlighted the greatest differences in the L group (Supplementary Fig. 7). In comparing RA from dnPI3K Tg(+/−) with Ntg, there was a downregulation in proteins associated with metabolic processes/pathways and tricarboxylic acid (TCA) cycle (Supplementary Fig. 5, Cluster-305) and an increase in proteins associated with protein localization/transport, regulation of actin cytoskeleton, and signaling (Rho GTPases and mitogen-activated protein kinase (MAPK)) (Supplementary Fig. 5, Cluster-310). The comparison of RA from dnPI3K Tg(+/−) and the subset of small atria from dnPI3K Tg(+/+) showed a downregulation of pathways associated with metabolic processes/metabolism, response to insulin (Supplementary Fig. 6, Cluster-604), and significant enrichment for mRNA splicing, splicesome, and programmed cell death (Supplementary Fig. 6, Cluster-603). The comparison of RA from the 3 dnPI3K Tg (+/+) subgroups demonstrated that the most striking differences were in the group with the largest atria. Consistent with the largest atria presenting with substantial fibrosis and in some cases thrombi, there was enrichment in pathways involved in elastic fiber formation, extracellular matrix organization, complement and coagulation cascades, and fibrin clot formation (Supplementary Fig. 7, Cluster-434). This was accompanied by a down regulation of pathways associated with muscle structure and contraction, metabolism, sarcomere organization, and signaling (calcium, Roundabout (ROBO) receptors, and cyclic guanosine monophosphate (cGMP)−protein kinase G (PKG)) (Supplementary Fig. 7, Cluster-435).

Trend-based expression analysis was performed to identify proteins that were increasing or decreasing in a dose−response manner based on pathology (from no pathology in Ntg atria through to the most pathology in dnPI3K Tg(+/+) atria L group; Fig. 4B and Supplementary Data File 2). The majority of proteins upregulated were within Cluster-723, highlighted by dysregulated extracellular matrix organization/structure and metabolic processing. Within the top 10 proteins differentially regulated in Cluster-723 across the genotypes, microfibril-associated glycoprotein 4 (MFAP4) and galectin-3 (LGALS3) (Supplementary Fig. 8) have previously been shown to have a functional role in regulating atrial pathology.[28,29] Expression of other proteins elevated or decreased in abundance associated with atrial pathology across the genotypes are presented in Supplementary Fig. 8.

Next, we performed a comparative analysis of proteins identified in mice atrial tissue with atrial tissue or plasma from patients with AF (proteomics data sets described in references [30−32])(Fig. 4H and Sheet 19 in Supplementary Data File 2). Fifty different proteins across the 3 main clusters (723−725) were co-identified in these studies associated with human AF (Supplementary Data File 2). Within Cluster-723 were extracellular matrix (ECM)-related proteins (MFAP4, EGF containing fibulin extracellular matrix protein 1 (EFEMP1), and fibulin 5 (FBLN5)), within Cluster 724 were contractile-related proteins myosin heavy chain 7 (MYH7) and ATPase Na^+/K^+ transporting subunit beta 1 (ATP1B1)), and within Cluster-725 were metabolism-related proteins (creatine kinase, M-type (CKM) and translational activator of cytochrome c oxidase I (TACO1)) (Supplementary Fig. 8).

3.7. Contribution of inflammatory signaling, GM3, and defective physiological signaling in mediating pathology in a model of extreme endurance swim exercise and dnPI3K Tg (+/+) mice

The atrial defects and pathological proteomic signature in the dnPI3K Tg(+/+) mice were relevant to previous work describing atrial pathology in mice undertaking extreme exercise. Unlike regular aerobic exercise, which activates the IGF1−PI3K−Akt pathway in the heart and is associated with a protective phenotype and favorable cardiac molecular signature,[13] extreme/intense endurance exercise has been associated with atrial enlargement, fibrosis, arrhythmia, and a pathological signature including enrichment of ECM and inflammatory pathways.[33] There is evidence of cross-talk between IGF1 and inflammatory pathways via GM3 ganglioside, a glycosphingolipid within cellular membranes. We previously found GM3 to be elevated in the atria of a mouse model with heart failure and AF.[34] Increased GM3 has been associated with defective IGF1R signaling, insulin resistance, and dysregulation of inflammatory pathways via Toll-like receptor (TLR) signaling.[34−36] Increased GM3 reduces membrane fluidity and disrupts the normal interaction of IGF1R with caveolins to induce downstream protective PI3K signaling. Here we investigated the potential contribution of these pathways in a setting of extreme exercise by mining a freely available microarray data set from atria of mice that had undergone intense swim training for 6 week and were shown to have atrial enlargement, fibrosis, and increased AF susceptibility.[33] An enrichment of genes involved with inflammatory pathways (including TLR4, nuclear factor kappa-light-chain-enhancer of activated B cells (NFκβ), and tumor necrosis factor alpha (TNFα)) was previously presented in a heatmap format[33] and is quantified by us in a graphical format here (Fig. 5A). In addition to this, we present previously unreported new data from the profiling data set, including an elevation of *ST3 beta-galactoside alpha-2,3-sialyltransferase 5* (*St3gal5*), the gene encoding GM3 synthase (GM3S; the enzyme responsible for GM3 production, Fig. 5A), as well as dysregulation of genes critical for physiological PI3K−Akt1−CCAAT/enhancer binding protein beta (C/EBPβ)−Cited4 signaling (Fig. 5B). Key differences in IGF1−PI3K signaling in the heart with aerobic swim training (green) and extreme exercise (red) are illustrated in Fig. 5C.

To assess whether GM3 and TLR4 may have contributed to the more severe pathological phenotype in the dnPI3K homozygote *vs*. heterozygote Tg, we assessed TLR4 gene expression by quantitative real-time polymerase chain reaction (qPCR) and GM3 lipids by mass spectrometry. TLR4 gene expression was elevated in hearts of dnPI3K Tg(+/−) *vs*. Ntg and elevated further in female dnPI3K Tg(+/+) *vs*. dnPI3K Tg (+/−) (Fig. 5D). By contrast, TLR4 gene expression was not different from Ntg in the caPI3K Tg models (Fig. 5D). PCA plots highlighted differences in the lipidome of ventricles and atria from Ntg and the dnPI3K Tg models (Supplementary Fig. 8). Total GM3 lipids were elevated in ventricle and atria tissue from both dnPI3K Tg models (Fig. 5E). In the caPI3K models there was a decrease or no change (Fig. 5E and Supplementary

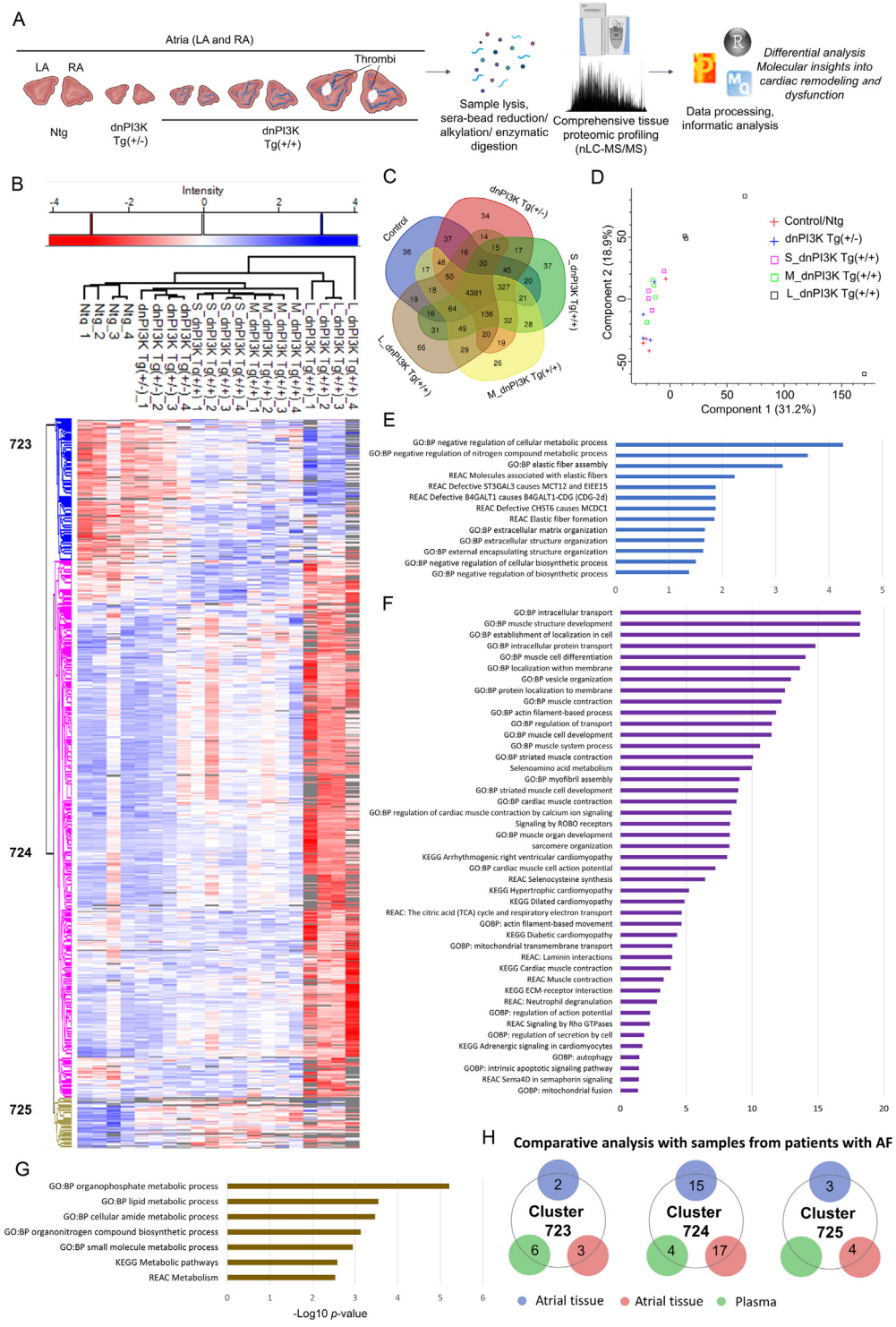

Fig. 4. Distinct regulation of the atrial proteome in female heterozygote and homozygote dnPI3K Tg mice and comparative analysis with the human AF proteome. (A) Schematic overview of atrial size in each mouse model and proteomic workflow. Blue lines within the atria highlight the presence of fibrosis in the homozygote dnPI3K Tg(+/+) mice. (B) Heatmap of significant proteins ($p < 0.01$ analysis of variance) in RA from female Ntg, dnPI3K Tg(+/−), and dnPI3K Tg(+/+) divided into 3 subsets based on atrial size (S = small, M = medium, L = large) (728 proteins); mice: ~20 week. $n = 4$/group. Proteins were identified in at least 70% of samples in at least 1 group. (C) Venn diagram of the number of proteins identified in each group $n = 4$ (Ntg/control: 5145, dnPI3K Tg(+/−): 5221, S_dnPI3K Tg (+/+): 5249, M_dnPI3K Tg(+/+): 5265, L_dnPI3K Tg(+/+): 4954). (D) PCA plot of valid values 70% cut off in at least 1 group across all groups. Based on the log2 intensity (LFQ) transformed value of all samples. Missing values were replaced by imputation from a normal distribution (downshift 1.8, width 0.3, Perseus). (E−G) Gene Ontology enrichment of Clusters 723, 724, and 725, respectively, GO:BP, KEGG, REAC using Gprofiler. −log10 *p*-value. (H) Comparative analysis venn diagram of shared proteins in each cluster across 3 human AF proteome studies (further details in Supplementary Data File 2). AF = atrial fibrillation; B4GALT1-CDG (CDG-2d) = beta-1,4-galactosyltransferase deficiency with carbohydrate deficient glycoprotein syndrome type IId; CHST6 = carbohydrate sulfotransferase 6; dnPI3K Tg(+/−) = heterozygote dominant-negative phosphoinositide 3-kinase mutant; dnPI3K Tg(+/+) = homozygote dominant-negative phosphoinositide 3-kinase mutant; EIEE15 = developmental and epileptic encephalopathy, 15; GO:BP = Gene Ontology: Biological Process; KEGG = Kyoto Encyclopedia

Data File 3). Given the elevation of GM3 in the dnPI3K Tg models, we interrogated the proteomic data further by performing informatic analysis and pathway network enrichment analysis for GM3-associated networks. STRING network analysis focusing on protein−protein interactions and their association with proteins associated with the GM3 synthase pathway is presented in Supplementary Fig. 9. This highlights proteins associated with GM3, of which 11 were identified in the current study, including proteins that were differentially regulated (archain 1 (ARCN1) and hexosaminidase subunit beta (HEXB); both $p < 0.05$) (Sheets 21−23 in Supplementary Data File 2).

3.8. Evidence of dysregulation of GM3 and PI3K-related lipids in veteran athletes with AF

Given the evidence of dysregulation of the PI3K signaling cascade in the atria of mice that had undergone extreme exercise training (Fig. 5B), together with pathology in dnPI3K Tg (+/+), we assessed whether there was any evidence of dysregulation in IGF1R−PI3K signaling in veteran athletes with AF by assessing plasma lipids. A description and comparison of athletes with and without AF is presented in Supplementary Table 12. All athletes were male, and age and fitness were comparable between groups. The 78 athletes (>40 years) had all been engaged in endurance sports for >10 years. Forest plot analysis highlighted key differences across the plasma lipidome in athletes with and without AF (Supplementary Fig. 10). We focused on lipids that feed into the production of GM3 lipids (e.g., dihexosylceramide (Hex2Cer)) with the capacity to disrupt IGF1R−PI3K signaling[34] as well as phosphatidylinositol monophosphate (PIP1) and lysophosphatidylinositol (LPI), which are regulators/constituents within the inositol−PI3K signaling network[37] (Fig. 6A and 6B and Supplementary Data File 3). In athletes with AF, total Hex2Cer, Hex3Cer, and GM3 lipids were elevated, PIP1 levels were lower, and LPI levels were higher *vs*. athletes without AF (Fig. 6C). Lipid ratios, which provide further insight into the regulation of lipid pathways, were also calculated.[38,39] Four lipid ratios related to the PI3K pathway had more significant *p* values than the individual total lipids alone (Fig. 6D *vs*. Fig. 6C). To ascertain the potential significance of PI3K-related lipids compared to other lipids (42 classes), we corrected lipids for age and calculated the *p* value of each lipid class, the *p* value of all lipid ratios, and the *p*-gain (p_{gain}) of the ratio *vs*. the individual lipid class.[39] Of the 6 lipid ratios from the total number of ratios (>800) with a $p_{gain} > 10$ (Supplementary Data File 3), 4 of the top 5 were related to the PI3K pathway (Fig. 6E and Supplementary Data File 3).

4. Discussion

Understanding the initiating molecular mechanisms underlying atrial enlargement, fibrosis, and atrial thrombi will be critical for preventing and treating AF. In this work, we demonstrated that reduced PI3K activity in homozygote dnPI3K mice was associated with atrial dysfunction, fibrosis, and increased susceptibility to atrial enlargement and thrombi, and we provided a resource of proteome signatures that were altered across a spectrum of atrial phenotypes. In contrast, we found no evidence of increased PI3K activity causing cardiac pathology. Further, our proteome comparative analysis between mice and humans identified proteins relevant to human AF, and we identified dysregulated lipid ratios related to the PI3K pathway in athletes with AF.

4.1. No evidence that PI3K activity within physiological levels leads to cardiac dysfunction, pathology, or arrhythmia

Heterozygote caPI3K Tg(+/−) mice have increased cardiac PI3K activity and develop physiological hypertrophy (i.e., normal heart function and no evidence of cell death or fibrosis).[23] In the current study, we generated caPI3K Tg(+/+) to increase cardiac PI3K activity further. Swimming or voluntary wheel running in mice for 4 week was previously shown to increase PI3K(p110α) activity in the heart ∼2-fold *vs*. untrained mice.[22] PI3K activity was elevated 2.9-fold in hearts of caPI3K Tg(+/−) and 5.1-fold in caPI3K Tg(+/+) *vs*. Ntg, and this was associated with a greater increase in heart weight in caPI3K Tg(+/+). Based on multiple measures, including AW and LW within a normal range, preserved cardiac function, regular ECG parameters, and absence of fibrosis, the hypertrophic response in caPI3K Tg(+/+) was characteristic of physiological hypertrophy. At the molecular level, cardiac expression of ANP, BNP, and collagen genes was comparable to Ntg or lower in caPI3K Tg(+/+), which is consistent with previous studies in caPI3K Tg(+/−) and/or exercise trained mice.[4,10,40] In comparing the homozygote caPI3K Tg model with previous IGF1−PI3K−Akt models presenting with evidence of cardiac dysfunction and pathology, there are some key differences. In IGF1 cardiac-specific Tg mice that developed pathological hypertrophy and atrial fibrosis over time, circulating IGF1 levels were elevated, which could contribute to secondary side effects in other cardiac cell types (e.g., fibroblasts leading to fibrosis).[20] Cardiac pathology was identified in an Akt model with very high transgene expression and Akt activity (80-fold higher than control mice)[41] as well as Akt models with inadequate angiogenesis.[13,42] An 80-fold increase in Akt activity is well above physiological levels; the phosphor-Akt/total Akt ratio is elevated ∼2-fold in the mouse heart with swim exercise.[4,43] The caPI3K Tg model does not display inadequate angiogenesis; in fact, angiogenesis was elevated in mice receiving a caPI3K gene therapy.[5] Within the current study, PI3K activity was chronically elevated in the hearts of caPI3K Tg models for ∼5 months. This is equivalent to ∼15 years in humans and demonstrates that mid- to long-term activation of this pathway is safe in the adult mouse heart.[44,45]

of Genes of Genomes; LFQ = label free quantitation; MCT12 = monocarboxylate transporter 12; MCDC1 = macular corneal dystrophy (a condition associated with CHST6 gene); nLC-MS/MS = nano liquid chromatography-tandem mass spectrometry; Ntg = non-transgenic; PCA = principal component analysis; RA = right atrium; REAC = Reactome; ST3GAL3 = ST3 beta-galactoside alpha-2,3-sialyltransferase 3.

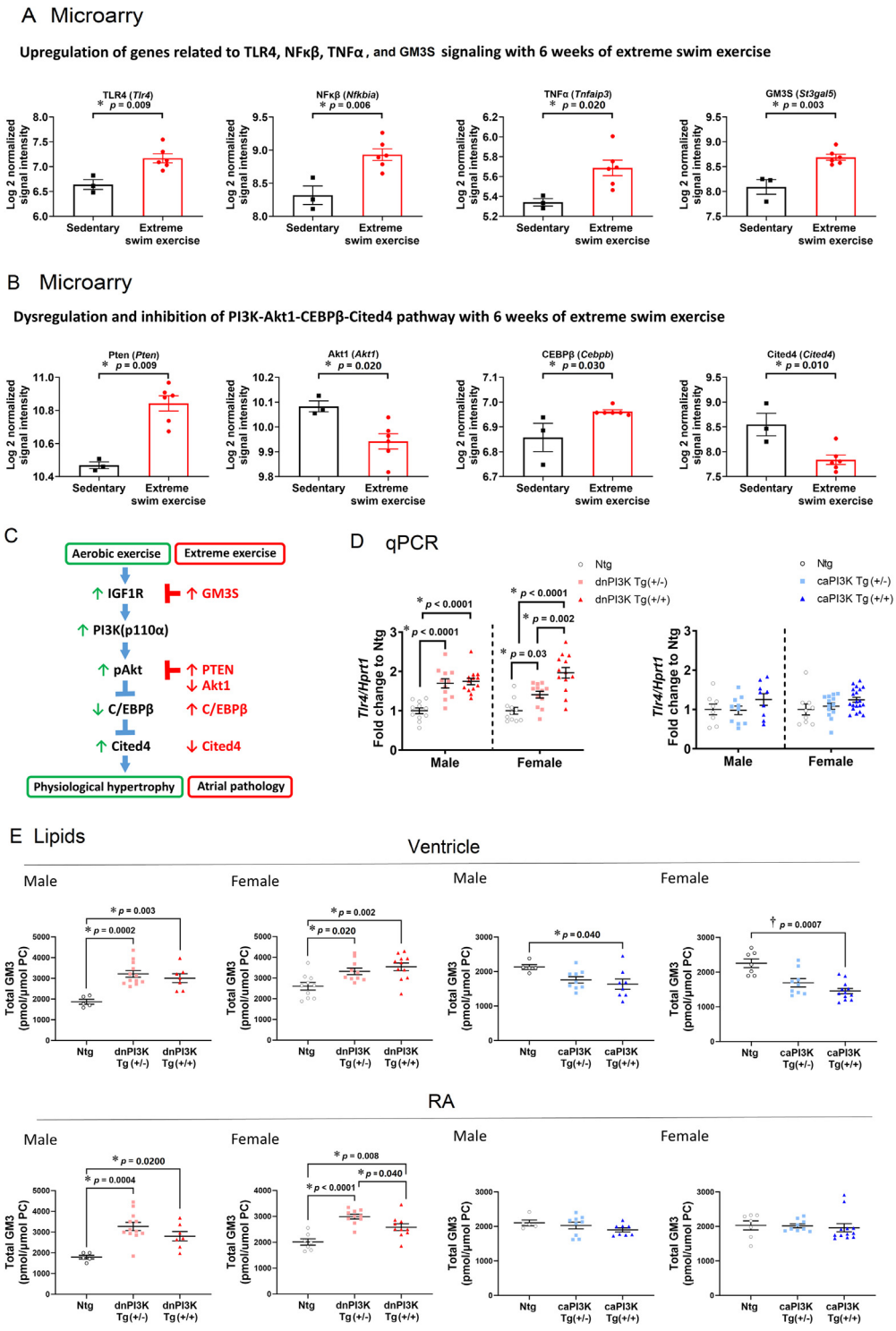

Fig. 5. Inflammatory signaling, GM3, and defective physiological signaling in a model of extreme endurance swim exercise and dnPI3K Tg(+/+) mice. (A) mRNAs related to TLR4 (*Tlr4*), NFκβ (*Nfkbia*), TNFα (*Tnfaip3*) signaling, and GM3 (GM3S gene expression, *St3gal5*), and (B) mRNAs related to the PI3K−Akt1−CEBPβ−Cited4 pathway by microarray in atria from sedentary mice ($n = 3$), and mice subjected to 6 week of extreme swim exercise ($n = 6$). Microarray deposited at https://www.ebi.ac.uk/arrayexpress/experiments/E-MTAB-3106/. (C) Schematic showing IGF1R−PI3K signaling in mice in response to aerobic swim training (green) and the differences with extreme swim exercise (red). (D) Gene expression by qPCR of *Tlr4* relative to *Hprt1* from ventricle tissue of 20-week-old dnPI3K Tg/caPI3K Tg mice and Ntg littermates: Ntg (male/female): $n = 11/11$, dnPI3K Tg(+/−): $n = 11/12$, dnPI3K Tg(+/+): $n = 13/13$; and caPI3K Tg mice: Ntg (male/female): $n = 8/9$, caPI3K Tg(+/−): $n = 10/13$, caPI3K Tg(+/+): $n = 9/20$. (E) Lipidomics was performed on ventricle and RA from 20-week-old dnPI3K Tg and Ntg littermates (male/female): Ntg: $n = 5/10$, dnPI3K Tg(+/−): $n = 12/10$, dnPI3K Tg(+/+): $n = 7/11$ (RA: female dnPI3K Tg(+/+): $n = 10$). For caPI3K Tg and Ntg littermates (male/female): Ntg: $n = 5/7$, caPI3K Tg(+/−): $n = 9/9$, caPI3K Tg(+/+): $n = 8/12$. Data points represent individual mice, presented as mean ± SEM. A and B: Unpaired *t* tests. D and E: * indicates one ay analysis of variance followed by Tukey's. †Kruskal-Wallis followed by Dunn's (data not normally distributed). Akt1 = AKT serine/threonine kinase 1; caPI3K Tg(+/−) = heterozygote constitutively activated phosphoinositide 3-kinase mutant; caPI3K

4.2. Reduced PI3K activity contributes to cardiac dysfunction, cardiac fibrosis, arrhythmia, and increased susceptibility to atrial thrombi

Heterozygous dnPI3K Tg were previously shown to have smaller hearts with relatively normal heart function, without evidence of cell death or fibrosis.[23] This phenotype has been reproducible within multiple laboratories worldwide for more than 20 years.[6,23,43,46] It therefore came as a surprise to identify atrial enlargement and thrombi in dnPI3K Tg within a more recent study. On further assessment, it became apparent there had been a breeding error, which led to the generation of both heterozygote and homozygote dnPI3K mice, and atrial enlargement and thrombi were only present in a subset of homozygote mice. Given this unexpected observation, it was important to assess whether this result was reproducible. In the current study, both heterozygote and homozygote dnPI3K Tg displayed a small heart phenotype that was comparable based on heart weight. However, dnPI3K Tg(+/+) displayed significant cardiac dysfunction and arrhythmia in comparison to Ntg and dnPI3K Tg(+/−), and atrial enlargement and thrombi were only present in dnPI3K Tg(+/+). Some of our prior studies had implicated a decrease in PI3K leading to an accelerated heart failure phenotype in settings of pressure overload, dilated cardiomyopathy (DCM), diabetic cardiomyopathy, and MI.[6,7,10,26] However, to our knowledge, our observations in homozygote dnPI3K Tg represents the first study to implicate a decrease in PI3K activity directly leading to severe cardiac dysfunction, serious ECG abnormalities, atrial enlargement, atrial fibrosis, and thrombi (i.e., in the absence of a cardiac stress/disease model). On expressing atrial weight relative to total heart weight, this ratio was not different between Ntg and dnPI3K Tg(+/−) but was substantially elevated in the dnPI3K Tg(+/+), highlighting a predominant atrial myopathy phenotype in dnPI3K Tg(+/+). Atrial pre-load (venous return) and ventricular systolic reserve were not assessed in the current study. However, reduced LA booster pump function in dnPI3K Tg(+/+) measured by echocardiography in the context of no difference in atrial after-load (ventricular end-diastolic pressure), together with a proteomic profile highlighting a downregulation of pathways associated with metabolism and muscle contraction, is indicative of reduced atrial contractility.[47] Despite no evidence of atrial myopathy in dnPI3K Tg (+/−) based on increased atrial weight, they also presented with evidence of atrial dysfunction on echocardiography. Evidence of atrial dysfunction *prior to* atrial enlargement has also been observed in humans (e.g., patients with hypertrophic cardiomyopathy and hypertension).[48] The current work identifying atrial enlargement and pathology in dnPI3K Tg(+/+) and atrial dysfunction in both dnPI3K Tg(+/−) and dnPI3K Tg (+/+) is significant because molecular mechanisms contributing to the initiation of atrial pathology and thrombi are not well understood.[3] This also has implications for the use of any drugs in the clinic that inhibit PI3K. PI3K inhibitors are being actively developed within the cancer field[49] with evidence of cardiotoxicity emerging.[50,51] We previously raised the concern of reduced PI3K activity in the context of pre-existing cardiac stress or pathology.[10,26,52] The current study indicates that a decrease in PI3K alone, in the absence of significant cardiac stress/pathology, can also lead to adverse outcomes. AF is often a condition of the aged. PI3K signaling is depressed/defective in settings of obesity, diabetes, and aging (all risk factors for AF).[53−55] This is likely to explain why mice with reduced cardiac PI3K displayed atrial pathology and arrhythmia by 20 week of age.

4.3. Atrial pathology progression and susceptibility to thrombi formation

To gain insight into the mechanisms underlying atrial pathology progression, we undertook proteomic profiling of 5 subsets of atria ranging from atria of normal size and function through to enlarged atria with thrombi. Using quantitative proteomics to identify proteins that were positively or negatively associated with atrial pathology, we identified proteins that have been previously linked with human AF (Supplementary Fig. 8) and/or shown to regulate atrial size (MFAP4 and LGALS3/Galectin-3).[28,29] MFAP4, which belongs to the fibrinogen-related protein superfamily, displayed a dose-dependent increase from Ntg through to the largest dnPI3K homozygote atria and was elevated in plasma of patients with AF.[56] More recently it was shown that angiotensin II-induced LA dilation, atrial fibrosis, and AF susceptibility were lower in MFAP4 knock out (KO) mice.[28] Galectin-3 expression was higher in the atria from the dnPI3K Tg(+/+) *vs*. dnPI3K Tg (+/−) and Ntg. Knockout of galectin-3 in mice was able to attenuate atrial enlargement and LV collagen content in a DCM Tg model.[29] Collectively, the proteomics analyses identified a number of proteins and networks related to defective cardiac contraction (calcium handling and myofibril proteins), mitochondrial function and metabolism, ECM homeostasis, and signaling (Supplementary Fig. 11). Each of these processes are interconnected (Supplementary Fig. 11), with defects in any single process contributing to defects in others. A number of these proteins have been previously identified in human data sets (Supplementary Fig. 11). We also identified proteins not previously directly linked with atrial pathology/AF, and this provides a resource for future work. A summary of key pathways regulated are provided in Fig. 7A.

Tg(+/+) = homozygote constitutively activated phosphoinositide 3-kinase mutant; CEBPβ = CCAAT/enhancer binding protein beta; Cited4 = Cbp/P300-interacting transactivator with Glu/Asp-rich carboxy-terminal Domain 4; dnPI3K Tg(+/−) = heterozygote dominant-negative phosphoinositide 3-kinase mutant; dnPI3K Tg(+/+) = homozygote dominant-negative phosphoinositide 3-kinase mutant; Hprt1= hypoxanthine phosphoribosyltransferase 1; IGF1R = insulin-like growth factor 1 receptor; NFκβ = nuclear factor kappa-light-chain-enhancer of activated B cells; Ntg = non-transgenic; PC = phosphatidylcholine; qPCR = quantitative polymerase chain reaction; PI3K = phosphoinositide 3-kinase; RA = right atrium; TLR4 = Toll-like receptor 4; TNFα = tumor necrosis factor alpha; GM3 = monosialodihexosylganglioside; GM3S = monosialodihexosylganglioside synthase .

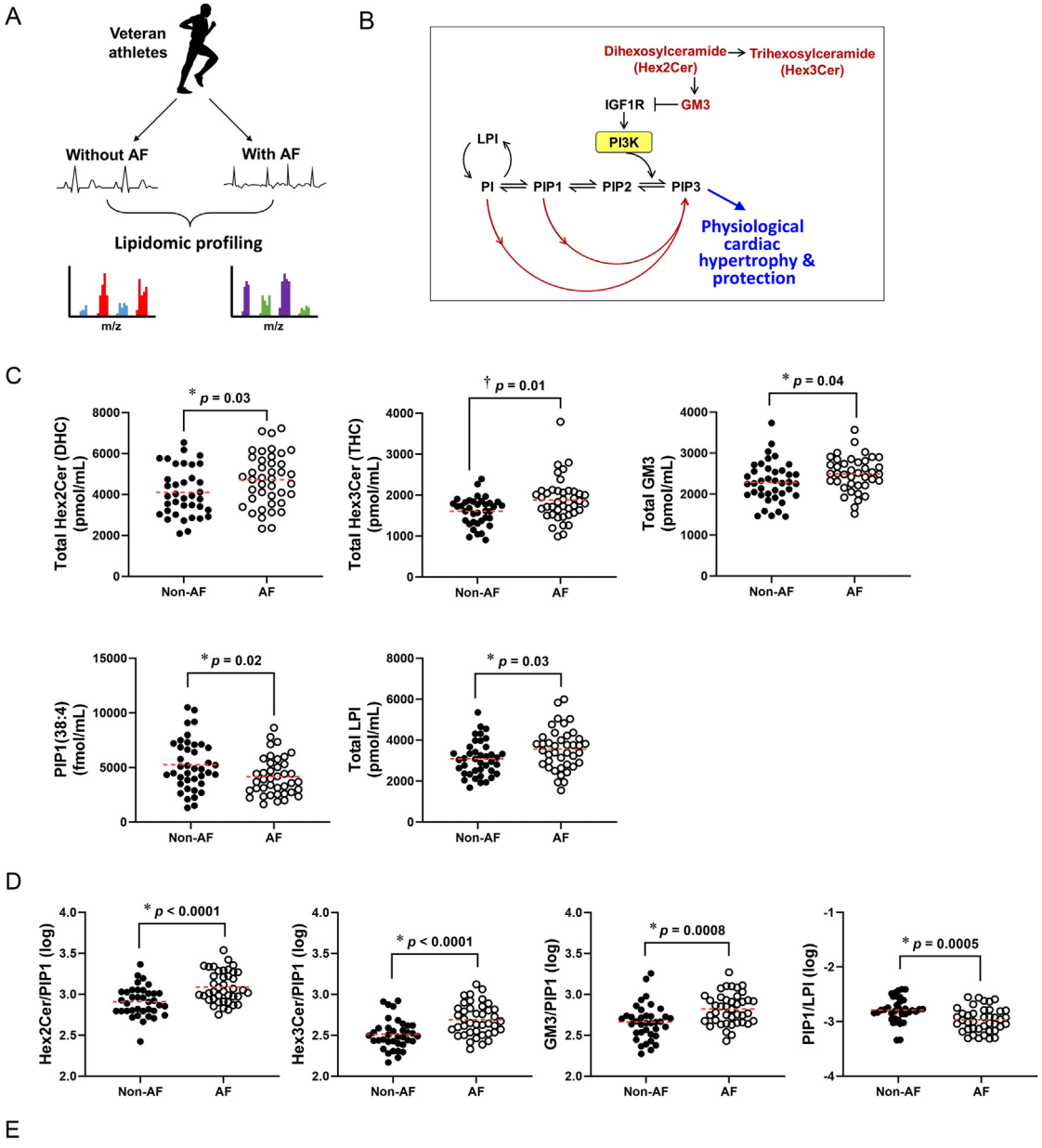

E

Lipid ratio	Lipid 1 *p*-value	Lipid 2 *p*-value	Ratio *p*-value	p_{gain}
Hex2Cer/PIP1	Hex2Cer=1.68E–02	PIP1=1.46E–02	5.11E–05	286.40
Hex3Cer/PIP1	Hex3Cer=6.29E–03	PIP1=1.46E–02	4.77E–05	131.71
GM3/PIP1	GM3=2.19E–02	PIP1=1.46E–02	7.78E–04	18.82
GM1/PIP1	GM1=4.21E–02	PIP1=1.46E–02	8.16E–04	17.94
PIP1/LPI	PIP1=1.46E–02	LPI=8.39E–03	4.68E–04	17.92

Fig. 6. Dysregulation of GM3 and PI3K-related lipids in veteran athletes with AF. (A) Lipidomics on plasma from veteran athletes with and without AF. (B) Relationship of PI species with PI3K and GM3 and ceramide lipid species. Changes in regulators of the pathway can impact PI3K and the formation of PIP3. (C) Total Hex2Cer (DHC), Hex3Cer (THC), GM3, PIP1, and LPI. (D) Most significant lipid ratios related to the PI3K pathway. Athletes without AF, $n = 37$; athletes with AF, $n = 41$. Data presented as scatter plots and mean. (E) Lipid ratios corrected for age with a $p_{gain} > 10$ (top 5 presented from the total number of ratios (>800); only 6 ratios had a $p_{gain} > 10$; Supplementary Data File 2). * indicates unpaired-test. † indicates Mann-Whitney *U* test (data not normally distributed). AF = atrial fibrillation; GM3 = monosialodihexosylganglioside; Hex2Cer (DHC) = dihexosylceramide; Hex3Cer (THC) = trihexosylceramide; IGF1R = insulin-like growth factor 1 receptor; LPI = lysophosphatidylinositol; m/z = mass-to-charge ratio; PI = phosphatidylinositol; PI3K = phosphoinositide 3-kinase; PIP = phosphatidylinositol monophosphate.

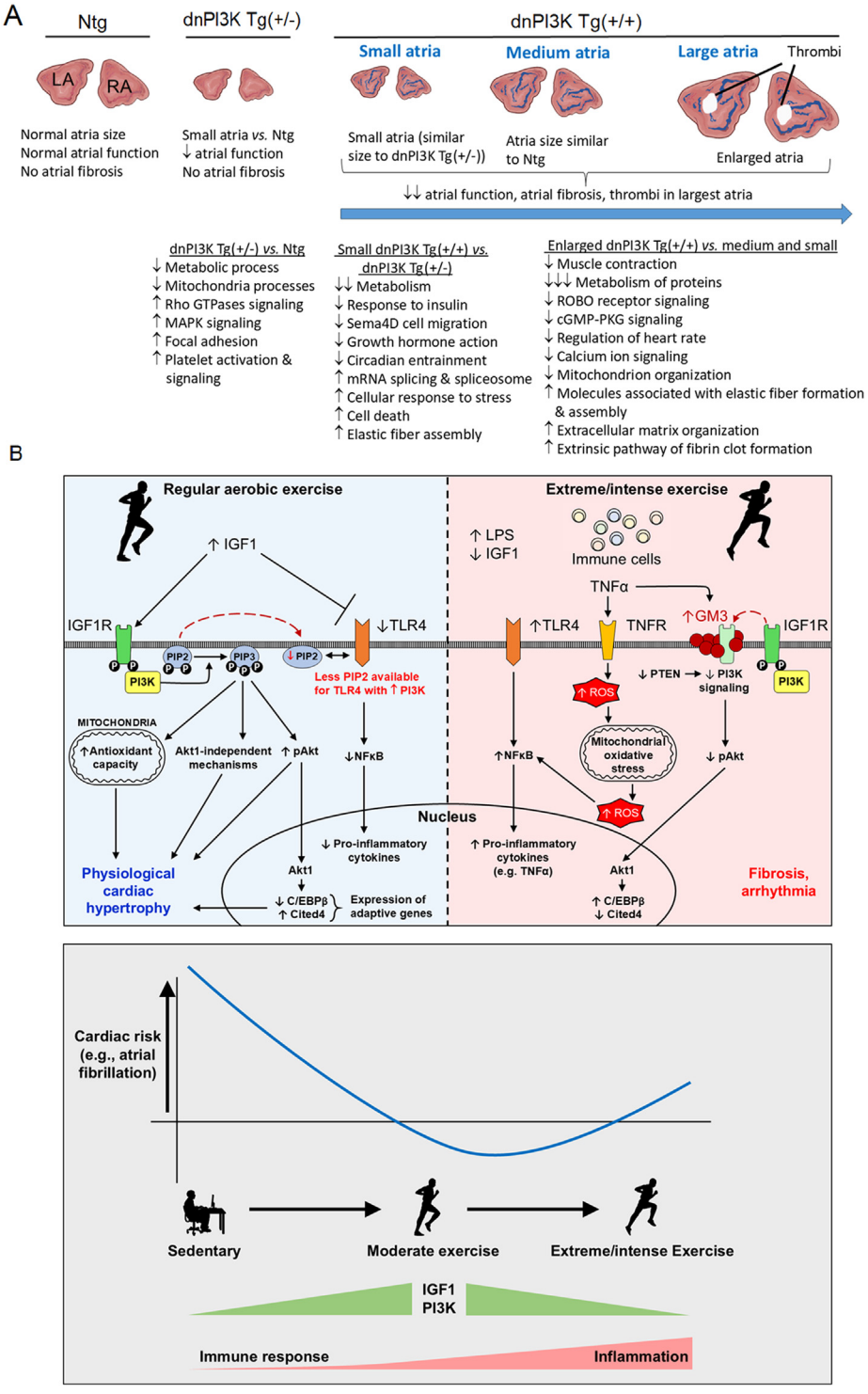

Fig. 7. Schematics highlighting cellular processes and signaling pathways during progression of atrial pathology, and regular aerobic exercise *vs*. Extreme/intense exercise. (A) Summary of differences in atrial size, function, fibrosis, and thrombi formation in Ntg, heterozygote dnPI3K Tg(+/−), and homozygote dnPI3K Tg (+/+). Cellular processes and signaling pathways dysregulated in the atria based on proteomics data. (B) Overview of IGF1−PI3K signaling in the heart with regular and extreme exercise (upper panel). IGF1 is elevated with regular exercise (left side, blue). In a setting of increased PI3K (exercise or caPI3K Tg), PIP2 is converted to PIP3, limiting the availability of PIP2 for TLR4 signaling and subsequently reducing pro-inflammatory cytokines. Extreme/intense exercise is associated with elevated LPS, lower IGF1, and increased TLR4 signaling (right side, red). There is also evidence of increased GM3 in response to increased TNFα, which would inhibit IGF1R−PI3K signaling. Increased GM3 reduces membrane fluidity and disrupts the normal interaction of IGF1R with caveolins to induce downstream protective PI3K signaling. Collectively these signaling alterations will contribute to cell death, fibrosis, and arrhythmia. Lower panel: Potential contribution of PI3K signaling to the reverse J-shaped relationship between physical activity and cardiac risk. An inverse relationship between PI3K activity and cardiac risk is hypothesized. Akt1 = AKT serine/threonine kinase 1; caPI3K Tg(+/−) = heterozygote constitutively activated phosphoinositide 3-kinase mutant; caPI3K Tg (+/+) = homozygote constitutively activated phosphoinositide 3-kinase mutant; C/EBPβ = CCAAT/enhancer binding protein beta; Cited4 = Cbp/P300-interacting

4.4. Potential role of defective IGF1R−PI3K signaling contributing to intense exercise-induced cardiac complications in humans

To date, there is limited knowledge regarding the molecular mechanisms responsible for increased cardiac risk with "too much" or "too little" exercise/physical activity. Previous work has implicated TNFα and p38 in mediating extreme exercise-induced atrial enlargement and remodeling in animals.[33] Wild-type mice subjected to extreme swimming/treadmill exercise (>70% of maximal oxygen consumption (VO_{2max})) for 6 week displayed atrial enlargement, fibrosis, inflammation, and elevated TNFα−NFκβ−p38 MAPK signaling. These features were partially prevented in TNFα KO mice or mice given a p38 inhibitor.[33] We previously reported that the phosphorylation of IGF1R and PI3K activity were lower in atrial appendages of patients with AF.[26,34] While it is well recognized that IGF1−PI3K−Akt1−CEBPβ−Cited4 signaling is elevated in the heart with regular aerobic exercise,[4,21,22] we present evidence here that this pathway is defective in the atria in a setting of extreme endurance exercise in mice (Fig. 5B and 5C). This is further supported by a study showing that IGF1 gene expression was lower in the atria of mice subjected to intense swim exercise for 2 week.[57]

To complement our mouse data showing reduced PI3K contributes to atrial pathology and arrhythmia, and to evaluate the potential relevance in humans, we assessed whether dysregulation IGF1−PI3K signaling was also a feature of humans with AF. Here we performed lipidomics analyses in a unique cohort of veteran athletes undertaking endurance sports with and without AF. Consistent with the idea that defective IGF1−PI3K signaling could contribute to atrial pathology, we show evidence of dysregulation of plasma lipids that feed into the PI3K pathway (including Hex2Cer, GM3, PIP1, and LPI) in athletes with AF. Further, on ranking lipid ratios using all total lipid species (>800 lipid ratios), the top 3 were related to the PI3K pathway.

4.5. Overview of IGF1−PI3K signaling with regular vs. extreme/intense exercise and inactivity

Based on previous studies and work presented here, we provide an overview of IGF1−PI3K signaling in the heart with regular aerobic exercise, intense exercise, and sedentary behavior. Circulating IGF1 levels increase in response to regular aerobic exercise, including increased cardiac IGF1 formation.[58−60] This activates cardiac PI3K signaling, which plays a role in the maintenance of cardiac structure, electrical function, cell survival, and antioxidant, anti-inflammatory, and anti-fibrotic properties[7,10,61,62] (Fig. 7B, upper left panel, blue). In contrast, intense exercise has been associated with increased lipopolysaccharide (LPS), reduced IGF1, upregulation of TLR signaling, activation and nuclear entry of NFκβ, and transcription of pro-inflammatory cytokines, including TNFα (Fig. 7B, upper right panel, red).[63] There is also evidence that TNFα induces an increase in gangliosides (including GM3), which contribute to defects in insulin signaling,[64] and that GM3 lipids can regulate TLR4 signaling.[36] We previously identified elevated GM3 lipids in atria from a mouse model with enlarged atria, arrhythmia, and increased susceptibility to AF.[34] Of note, both regular aerobic exercise and extreme/intense exercise induce an immune response. However, intense exercise has been associated with higher levels of inflammatory mediators, which can lead to cardiac pathology when endogenous protective mechanisms are overwhelmed. Prior work suggests that PI3K inhibits cardiac inflammation and fibrosis by inhibiting TLR4 signaling,[65] potentially via a mechanism involving phosphatidylinositol 4,5-bisphosphate (PIP2, a shared substrate of PI3K and TLR4)[66] (Fig. 7B, upper left panel). Studying signaling mechanisms within sedentary/inactive mice is complex, as any voluntary physical activity will increase PI3K in the heart. However, findings from a low capacity running (LCR) rat model are consistent with reduced cardiac PI3K contributing to cardiac pathology due to physical inactivity. LCR rats have low intrinsic exercise capacity and increased cardiovascular risk profile.[67] LVs from LCR rats showed reduced cardiac mitochondrial capacity and cardiomyocyte abnormalities (dysfunction and defective contractile kinetics), which were not apparent in myocytes from LCR treated with a PI3K activator.[68]

4.6. Study limitations

There are some limitations in the study. (a) It will be important to assess whether the PI3K-related lipids identified in athletes with AF can be validated in an independent cohort including females. (b) We identified novel protein signatures in atria from our dnPI3K models, which will require mechanistic studies to demonstrate whether they play key roles in regulating atrial size, fibrosis, and dysfunction. However, we are confident in the proteome resource we provide for the research community, given we identified a number of proteins previously shown to contribute to AF and that are relevant to human AF (Supplementary Fig. 11). (c) We cannot exclude the possibility that longer and/or higher PI3K activity (>10 fold) could lead to cardiac pathology. Aged caPI3K mice (20 months old) showed a subtle decline in fractional shortening (Ntg: 44.7% ± 0.9% *vs.* caPI3K: 42.6% ± 0.6%, mean ± SEM).[44] In considering therapeutic

transactivator with Glu/Asp-rich carboxy-terminal domain 4; cGMP = cyclic guanosine monophosphate; dnPI3K Tg(+/−) = heterozygote dominant-negative phosphoinositide 3-kinase mutant; dnPI3K Tg(+/+) = homozygote dominant-negative phosphoinositide 3-kinase mutant; GM3 = monosialodihexosylganglioside; IGF1R = insulin-like growth factor 1 receptor; LA = left atrium; LPS = lipopolysaccharide; NFκβ = nuclear factor kappa-light-chain-enhancer of activated B cell; Ntg = non-transgenic; ROS = reactive oxygen species; pAkt = phosphorylated Akt; qPCR = quantitative polymerase chain reaction; PI3K = phosphoinositide 3-kinase; PIP2 = phosphatidylinositol 4,5-bisphosphate; PKG = protein kinase G; PTEN = phosphatase and tensin homolog deleted on chromosome 10; RA = right atrium; ROBO = roundabout; TLR4 = Toll-like receptor 4; TNFα = tumor necrosis factor-alpha.

approaches targeting PI3K or other regulators of exercise-induced protection, it would be important to target a physiological range and monitor for any adverse consequences with chronic use. (d) Multiple mechanisms and factors will contribute to atrial and ventricular pathology with elevated cardiac risk in sedentary individuals and extreme endurance athletes.[17,19] Changes in cardiac PI3K alone will not completely recapitulate what is observed in humans. However, because PI3K is increased in the heart by physical activity/exercise, and is a master regulator of exercise-induced hypertrophy and protection, reduced PI3K is likely to contribute to increased cardiac risk.[4,5] (e) The contribution of GM3 requires further study. GM3 was comparably elevated in the atria of both heterozygote and homozygote mice, suggesting it may have contributed to atrial dysfunction in both models but not directly to atrial fibrosis, enlargement, and thrombi formation in the homozygote model. (f) It was not possible to directly assess PI3K activity in the atria of the extreme endurance exercise mouse model or subject caPI3K mice to this extreme exercise model. In support of reduced physiological PI3K signaling in a setting of extreme exercise, 4 week of excessive exercise in zebrafish was associated with heart enlargement, contractile impairment, mitochondrial abnormalities, elevated expression of ANP, BNP, and βMHC, together with a fall in pik3r1/PI3K.[69] Consistent with the idea of increased PI3K providing protection within the atria, we previously reported that the caPI3K transgene provided protection in a mouse model of DCM with atrial enlargement and fibrosis. Atria from caPI3K-DCM mice displayed less fibrosis than the DCM model alone.[26]

5. Conclusion

In summary, a reduction in PI3K in the mouse heart led to cardiac dysfunction, fibrosis, arrhythmia, and increased susceptibility to atrial enlargement and thrombi. In contrast, elevated PI3K was associated with a dose-dependent increase in heart size and preserved/enhanced cardiac function. Dysregulation of GM3 and PI3K-related lipids were identified in atria from mice with reduced PI3K and the plasma of athletes with AF. Proteomics of atrial tissue from dnPI3K Tg with varying degrees of atrial pathology identified dysregulation of multiple pathways related to metabolism, mitochondria, platelet signaling, response to insulin, and regulation of matrix organization and clot formation. Our murine proteome landscape is supported by co-identification of proteins from atrial tissue/plasma from humans with AF. This work advances our understanding of mechanisms underlying atrial pathophysiology and offers new avenues for therapeutic approaches. The work also supports further investigation of PI3K-related lipids as potential markers for identifying individuals at risk of AF, including athletes undertaking extreme endurance exercise and patients receiving cancer therapies that inhibit PI3K. There is increasing recognition that "clinical lipidomics" provides an opportunity to identify new predictive markers of cardiac pathology beyond triglycerides and cholesterol with economical value.[70]

Authors' contributions

SBS conducted experiments, acquired data, analyzed data, and wrote the manuscript; BCB was involved in student supervision, conducting experiments, acquiring data, and analyzing data; GSY, AM, HK, CAH, LB, DGD, AAD JHC, GWM, YKT conducted experiments, acquired data, and analyzed data; ME conducted experiments and acquired data; EIM conducted experiments and analyzed data; CMKT, RC, and GO analyzed data; JYYO participated method design and analyzing data; JL conducted experiments; NAM participated lipidomics methods and validation; KJ was responsible for human data collection and analysis; EJH was involved in human data collection and interpretation; CEH was involved in research proposal funding and intellectual input; RCYL acquired and analyzed data; CJT was responsible for student supervision and intellectual input; ACP provided resources; THM and H Kawakami participated data interpretation and intellectual input; PJM was responsible for lipidomics methods and interpretation; DWG was involved in resources, data interpretation and analysis; KLW took the responsibility of student supervision, acquiring data, analyzing data; ALG led on human study, data collection, analysis and interpretation; JRM was responsible for designing research studies, student supervision, research proposal funding, conducting experiments, acquiring data, analyzing data, and writing the manuscript. All authors contributed to the editing of the manuscript. All authors have read and approved the final version of the manuscript, and agree with the order of presentation of the authors.

Competing interests

The authors declare that they have no competing interests.

Acknowledgments

The authors wish to thank Yi Ching Chen, Gizem Sen, Teleah Belkin, Esther Boey, Natalie Patterson, and Amy Mitchell for their technical assistance. We acknowledge the use of facilities and technical assistance from the Monash Histology Platform, Australia. This work was supported by grants from NHMRC (Grant No. 1125514 and 2029334 to JRM, and 1120129 to JRM and CEH), National Heart Foundation of Australia (Vanguard-105720), and in part by the Victorian Government's Operational Infrastructure Support Program. SBS was supported by a joint Baker Heart and Diabetes Institute−La Trobe University doctoral scholarship. EJH, KLW, and ALG are supported by Future Leader Fellowships from the National Heart Foundation of Australia (Grant No.102536 to EJH, 102539 to KLW, and 102206 to ALG). BCB was supported by an Alice Baker and Eleanor Shaw Fellowship (The Baker Foundation, Australia). JRM was supported by a NHMRC Senior Research (Grant No. 1078985), Baker Fellowship (The Baker Foundation, Australia), and Cardiovascular Research Capacity Program−Research Leadership Grants (NSW Health).

Supplementary materials

Supplementary material associated with this article can be found in the online version at doi:10.1016/j.jshs.2025.101023.

References

1. Elliott AD, Middeldorp ME, Van Gelder IC, Albert CM, Sanders P. Epidemiology and modifiable risk factors for atrial fibrillation. *Nat Rev Cardiol* 2023;**20**:429. doi:10.1038/s41569-023-00834-w.
2. Kornej J, Börschel CS, Benjamin EJ, Schnabel RB. Epidemiology of atrial fibrillation in the 21st century: Novel methods and new insights. *Circ Res* 2020;**127**:4–20.
3. Chen YC, Voskoboinik A, Gerche AL, Marwick TH, McMullen JR. Prevention of pathological atrial remodeling and atrial fibrillation: *JACC* State-of-the-Art review. *J Am Coll Cardiol* 2021;**77**:2846–64.
4. McMullen JR, Shioi T, Zhang L, et al. Phosphoinositide 3-kinase (p110alpha) plays a critical role for the induction of physiological, but not pathological, cardiac hypertrophy. *Proc Natl Acad Sci U S A* 2003;**100**:12355–60.
5. Weeks KL, Gao X, Du XJ, et al. Phosphoinositide 3-kinase p110alpha is a master regulator of exercise-induced cardioprotection and PI3K gene therapy rescues cardiac dysfunction. *Circ Heart Fail* 2012;**5**:523–34.
6. Lin RCY, Weeks KL, Gao XM, et al. PI3K(p110alpha) protects against myocardial infarction-induced heart failure: PI3K-regulated miRNA and mRNA. *Arterioscler Thromb Vasc Biol* 2010;**30**:724–32.
7. Ritchie RH, Love JE, Huynh K, et al. Enhanced phosphoinositide 3-kinase (p110alpha) activity prevents diabetes-induced cardiomyopathy and superoxide generation in a mouse model of diabetes. *Diabetologia* 2012;**55**:3369–81.
8. Prakoso D, De Blasio MJ, Qin C, et al. Phosphoinositide 3-kinase (p110alpha) gene delivery limits diabetes-induced cardiac NADPH oxidase and cardiomyopathy in a mouse model with established diastolic dysfunction. *Clin Sci (Lond)* 2017;**131**:1345–60.
9. Prakoso D, De Blasio MJ, Tate M, et al. Gene therapy targeting cardiac phosphoinositide 3-kinase (p110alpha) attenuates cardiac remodeling in type 2 diabetes. *Am J Physiol Heart Circ Physiol* 2020;**318**:H840–52.
10. McMullen JR, Amirahmadi F, Woodcock EA, et al. Protective effects of exercise and phosphoinositide 3-kinase(p110alpha) signaling in dilated and hypertrophic cardiomyopathy. *Proc Natl Acad Sci U S A* 2007;**104**:612–7.
11. Fleg JL, Cooper LS, Borlaug BA, et al. Exercise training as therapy for heart failure: Current status and future directions. *Circ Heart Fail* 2015;**8**:209–20.
12. Boden WE, Franklin B, Berra K, et al. Exercise as a therapeutic intervention in patients with stable ischemic heart disease: An underfilled prescription. *Am J Med* 2014;**127**:905–11.
13. Bernardo BC, Ooi JYY, Weeks KL, Patterson NL, McMullen JR. Understanding key mechanisms of exercise-induced cardiac protection to mitigate disease: Current knowledge and emerging concepts. *Physiol Rev* 2018;**98**:419–75.
14. Buckley BJR, Lip GYH, Thijssen DHJ. The counterintuitive role of exercise in the prevention and cause of atrial fibrillation. *Am J Physiol Heart Circ Physiol* 2020;**319**:H1051–8.
15. Eijsvogels TMH, Thompson PD, Franklin BA. The "extreme exercise hypothesis": Recent findings and cardiovascular health implications. *Curr Treat Options Cardiovasc Med* 2018;**20**:84. doi:10.1007/s11936-018-0674-3.
16. La Gerche A, Heidbuchel H. Can intensive exercise harm the heart? You can get too much of a good thing. *Circulation* 2014;**130**:992–1002.
17. Guasch E, Mont L. Diagnosis, pathophysiology, and management of exercise-induced arrhythmias. *Nat Rev Cardiol* 2017;**14**:88–101.
18. Merghani A, Malhotra A, Sharma S. The U-shaped relationship between exercise and cardiac morbidity. *Trends Cardiovasc Med* 2016;**26**:232–40.
19. Guasch E, Benito B, Qi X, et al. Atrial fibrillation promotion by endurance exercise: Demonstration and mechanistic exploration in an animal model. *J Am Coll Cardiol* 2013;**62**:68–77.
20. Delaughter MC, Taffet GE, Fiorotto ML, Entman ML, Schwartz RJ. Local insulin-like growth factor I expression induces physiologic, then pathologic, cardiac hypertrophy in transgenic mice. *FASEB J* 1999;**13**:1923–9.
21. Weeks KL, Tham YK, Yildiz SG, et al. FoxO1 is required for physiological cardiac hypertrophy induced by exercise but not by constitutively active PI3K. *Am J Physiol Heart Circ Physiol* 2021;**320**:H1470–85.
22. Perrino C, Naga Prasad SV, Mao L, et al. Intermittent pressure overload triggers hypertrophy-independent cardiac dysfunction and vascular rarefaction. *J Clin Invest* 2006;**116**:1547–60.
23. Shioi T, Kang PM, Douglas PS, et al. The conserved phosphoinositide 3-kinase pathway determines heart size in mice. *EMBO J* 2000;**19**:2537–48.
24. McMullen JR, Shioi T, Zhang L, et al. Phosphoinositide 3-kinase (p110alpha) plays a critical role for the induction of physiological, but not pathological, cardiac hypertrophy. *Proc Natl Acad Sci U S A* 2003;**100**:12355–60.
25. Weeks KL, Henstridge DC, Salim A, Shaw JE, Marwick TH, McMullen JR. CORP: Practical tools for improving experimental design and reporting of laboratory studies of cardiovascular physiology and metabolism. *Am J Physiol Heart Circ Physiol* 2019;**317**:H627–39.
26. Pretorius L, Du XJ, Woodcock EA, et al. Reduced phosphoinositide 3-kinase (p110alpha) activation increases the susceptibility to atrial fibrillation. *Am J Pathol* 2009;**175**:998–1009.
27. Goodwin LO, Splinter E, Davis TL, et al. Large-scale discovery of mouse transgenic integration sites reveals frequent structural variation and insertional mutagenesis. *Genome Res* 2019;**29**:494–505.
28. Wang H, Liu M, Wang X, Shuai W, Fu H. MFAP4 deletion attenuates the progression of angiotensin II-induced atrial fibrosis and atrial fibrillation. *Europace* 2022;**24**:340–7.
29. Nguyen MN, Ziemann M, Kiriazis H, et al. Galectin-3 deficiency ameliorates fibrosis and remodeling in dilated cardiomyopathy mice with enhanced Mst1 signaling. *Am J Physiol Heart Circ Physiol* 2019;**316**:H45–60.
30. Chen HX, Li MY, Jiang YY, et al. Role of the PPAR pathway in atrial fibrillation associated with heart valve disease: Transcriptomics and proteomics in human atrial tissue. *Signal Transduct Target Ther* 2020;**5**:4. doi:10.1038/s41392-019-0093-2.
31. Liu Y, Bai F, Tang Z, Liu N, Liu Q. Integrative transcriptomic, proteomic, and machine learning approach to identifying feature genes of atrial fibrillation using atrial samples from patients with valvular heart disease. *BMC Cardiovasc Disord* 2021;**21**:52. doi:10.1186/s12872-020-01819-0.
32. Norby FL, Tang W, Pankow JS, et al. Proteomics and risk of atrial fibrillation in older adults (from the atherosclerosis risk in communities (ARIC) study). *Am J Cardiol* 2021;**161**:42–50.
33. Aschar-Sobbi R, Izaddoustdar F, Korogyi AS, et al. Increased atrial arrhythmia susceptibility induced by intense endurance exercise in mice requires TNFα. *Nat Commun* 2015;**6**:6018. doi:10.1038/ncomms7018.
34. Sapra G, Tham YK, Cemerlang N, et al. The small-molecule BGP-15 protects against heart failure and atrial fibrillation in mice. *Nat Commun* 2014;**5**:5705. doi:10.1038/ncomms6705.
35. Prokazova NV, Samovilova NN, Gracheva EV, Golovanova NK. Ganglioside GM3 and its biological functions. *Biochemistry (Mosc)* 2009;**74**:235–49.
36. Kanoh H, Nitta T, Go S, et al. Homeostatic and pathogenic roles of GM3 ganglioside molecular species in TLR4 signaling in obesity. *EMBO J* 2020;**39**:e101732. doi:10.15252/embj.2019101732.
37. Sasaki T, Takasuga S, Sasaki J, et al. Mammalian phosphoinositide kinases and phosphatases. *Prog Lipid Res* 2009;**48**:307–43.
38. Beyene HB, Olshansky G, T Smith AA, et al. High-coverage plasma lipidomics reveals novel sex-specific lipidomic fingerprints of age and BMI: Evidence from two large population cohort studies. *PLoS Biol* 2020;**18**:e3000870. doi:10.1371/journal.pbio.3000870.
39. Petersen AK, Krumsiek J, Wägele B, et al. On the hypothesis-free testing of metabolite ratios in genome-wide and metabolome-wide association studies. *BMC Bioinformatics* 2012;**13**:120. doi:10.1186/1471-2105-13-120.
40. McMullen JR, Shioi T, Huang WY, et al. The insulin-like growth factor 1 receptor induces physiological heart growth via the phosphoinositide 3-kinase(p110alpha) pathway. *J Biol Chem* 2004;**279**:4782–93.
41. Shioi T, McMullen JR, Kang PM, et al. Akt/protein kinase B promotes organ growth in transgenic mice. *Mol Cell Biol* 2002;**22**:2799–809.

42. Shiojima I, Sato K, Izumiya Y, et al. Disruption of coordinated cardiac hypertrophy and angiogenesis contributes to the transition to heart failure. *J Clin Invest* 2005;**115**:2108–18.
43. O'Neill BT, Kim J, Wende AR, et al. A conserved role for phosphatidylinositol 3-kinase but not Akt signaling in mitochondrial adaptations that accompany physiological cardiac hypertrophy. *Cell Metab* 2007;**6**:294–306.
44. Niizuma S, Inuzuka Y, Okuda J, et al. Effect of persistent activation of phosphoinositide 3-kinase on heart. *Life Sci* 2012;**90**:619–28.
45. Dutta S, Sengupta P. Men and mice: Relating their ages. *Life Sci* 2016;**152**:244–8.
46. Crackower MA, Oudit GY, Kozieradzki I, et al. Regulation of myocardial contractility and cell size by distinct PI3K-PTEN signaling pathways. *Cell* 2002;**110**:737–49.
47. Baysan O, Ocaklı E, Altuner T, Kocaman SA. Atria: A comprehensive evaluation with echocardiography. *Heart, Vessels and Transplantation* 2017;**1**:11–9.
48. Zhou D, Yang W, Yang Y, et al. Left atrial dysfunction may precede left atrial enlargement and abnormal left ventricular longitudinal function: A cardiac MR feature tracking study. *BMC Cardiovasc Disord* 2022;**22**:99. doi:10.1186/s12872-022-02532-w.
49. Cohen P, Cross D, Jänne PA. Kinase drug discovery 20 years after imatinib: Progress and future directions. *Nat Rev Drug Discov* 2021;**20**:551–69.
50. Dreyling M, Morschhauser F, Bouabdallah K, et al. Phase II study of copanlisib, a PI3K inhibitor, in relapsed or refractory, indolent or aggressive lymphoma. *Ann Oncol* 2017;**28**:2169–78.
51. Kim RD, Alberts SR, Peña C, et al. Phase I dose−escalation study of copanlisib in combination with gemcitabine or cisplatin plus gemcitabine in patients with advanced cancer. *Br J Cancer* 2018;**118**:462–70.
52. McMullen JR, Jay PY. PI3K(p110alpha) inhibitors as anti-cancer agents: Minding the heart. *Cell Cycle* 2007;**6**:910–3.
53. Fink RI, Kolterman OG, Griffin J, Olefsky JM. Mechanisms of insulin resistance in aging. *J Clin Invest* 1983;**71**:1523–35.
54. Tsang A, Hausenloy DJ, Mocanu MM, Carr RD, Yellon DM. Preconditioning the diabetic heart: The importance of Akt phosphorylation. *Diabetes* 2005;**54**:2360–4.
55. Kahn BB, Flier JS. Obesity and insulin resistance. *J Clin Invest* 2000;**106**:473–81.
56. Zhang X, Li H, Kou W, et al. Increased plasma microfibrillar-associated protein 4 is associated with atrial fibrillation and more advanced left atrial remodelling. *Arch Med Sci* 2019;**15**:632–40.
57. Oh Y, Yang S, Liu X, et al. Transcriptomic bioinformatic analyses of atria uncover involvement of pathways related to strain and post-translational modification of collagen in increased atrial fibrillation vulnerability in intensely exercised mice. *Front Physiol* 2020;**11**:605671. doi:10.3389/fphys.2020.605671.
58. Neri Serneri GG, Boddi M, Modesti PA, et al. Increased cardiac sympathetic activity and insulin-like growth factor-1 formation are associated with physiological hypertrophy in athletes. *Circ Res* 2001;**89**:977–82.
59. Cavalcante PAM, Gregnani MF, Henrique JS, Ornellas FH, Araújo RC. Aerobic but not resistance exercise can induce inflammatory pathways via Toll-like 2 and 4: A systematic review. *Sports Med Open* 2017;**3**:42. doi:10.1186/s40798-017-0111-2.
60. Berg U, Bang P. Exercise and circulating insulin-like growth factor 1. *Horm Res* 2004;**62**. Suppl. 1S50-8.
61. Waardenberg AJ, Bernardo BC, Ng DCH, et al. Phosphoinositide 3-kinase (PI3K(p110alpha)) directly regulates key components of the Z-disc and cardiac structure. *J Biol Chem* 2011;**286**:30837–46.
62. Yang KC, Foeger NC, Marionneau C, Jay PY, McMullen JR, Nerbonne JM. Homeostatic regulation of electrical excitability in physiological cardiac hypertrophy. *J Physiol* 2010;**588**:5015–32.
63. La Gerche A, Inder WJ, Roberts TJ, Brosnan MJ, Heidbuchel H, Prior DL. Relationship between inflammatory cytokines and indices of cardiac dysfunction following intense endurance exercise. *PLoS One* 2015;**10**:e0130031. doi:10.1371/journal.pone.0130031.
64. Sasaki N, Itakura Y, Toyoda M. Gangliosides contribute to vascular insulin resistance. *Int J Mol Sci* 2019;**20**:1819. doi:10.3390/ijms20081819.
65. Liu F, Wen Y, Kang J, et al. Regulation of TLR4 expression mediates the attenuating effect of erythropoietin on inflammation and myocardial fibrosis in rat heart. *Int J Mol Med* 2018;**42**:1436–44.
66. Laird MH, Rhee SH, Perkins DJ, et al. TLR4/MyD88/PI3K interactions regulate TLR4 signaling. *J Leukoc Biol* 2009;**85**:966–77.
67. Wisløff U, Najjar SM, Ellingsen O, et al. Cardiovascular risk factors emerge after artificial selection for low aerobic capacity. *Science* 2005;**307**:418–20.
68. Moreira JBN, Alves MNM, Britton SL, Koch LG, Wisloff U, Bye A. PI3K modulates cardiomyocyte phenotype in rats selected for low aerobic capacity. *Eur Heart J* 2013;**34**:4202. doi:10.1093/eurheartj/eht309.P4202. Suppl. 1.
69. Zhou Z, Zheng L, Tang C, et al. Identification of potentially relevant genes for excessive exercise-induced pathological cardiac hypertrophy in zebrafish. *Front Physiol* 2020;**11**:565307. doi:10.3389/fphys.2020.565307.
70. Vvedenskaya O, Holčapek M, Vogeser M, Ekroos K, Meikle PJ, Bendt AK. Clinical lipidomics—A community-driven roadmap to translate research into clinical applications. *J Mass Spectrom Adv Clin Lab* 2022;**24**:1–4.